ELECTROLYTE – SEMICONDUCTOR COMBINATIONS FOR ORGANIC ELECTRONIC DEVICES

Elias Said

Norrköping 2009

*To my parents**: David** and **Sara***

Electrolyte – Semiconductor Combinations for Organic Electronic Devices

Elias Said

Cover picture: Solutions of organic materials that were used in this thesis. From left to right: PSSH, PSSNa, PEDOT:PSS and P3HT. The inset shows the electric-field visualization (left) and the transistor (right) devices.

Linköping Studies in Science and Technology. Dissertations, No. 1228

Printed in Sweden by LiU-Tryck, Linköping, Sweden, 2009
ISBN: 978-91-7393-735-1
ISSN: 0345-7524

Abstract

The discovery of semi-conducting organic materials has opened new possibilities for electronic devices and systems because of their solution processibility, lightweight and flexibility compared to inorganic semiconductors. The combination of semiconductors with electrolytes, and more especially organic semiconductors and solid electrolytes has attracted the attention of researchers because of the multiple phenomena originating from the simultaneous motion of electrons and ions.

This thesis deals with organic-based devices whose working mechanism involves electrolytes. By measuring electrochromism induced by the field in isolated segments of conjugated polymer films, which is in contact with an electrolyte, the direction and the magnitude of the electric field along an electrolyte is quantified (paper I). In addition, using a polyanionic proton conductor in organic field-effect transistor (OFET) as gate dielectric results in low operation voltage and fast response thanks to the high capacitance of the electric double layer (EDLC) that is formed at organic semiconductor/ polyelectrolyte interface (paper III). Because an electrolyte is used as a gate insulator, the effect of the ionic currents on the performance of an EDLC-OFET has been investigated by varying the relative humidity of the device ambience (paper IV). Since the EDLC-OFET and the electrochromic display cell both are operated at low voltages, the transistor has been monolithically integrated with an electrochromic pixel, i.e. combining a solid state device and an electrochemical device (paper V). Further, a theoretical study of the electrostatic potential within a so called *pen*-heterojunction made up of two semi-infinite, doped semiconductor media separated by an electrolyte region is reported (paper II).

Populärvetenskaplig sammanfattning

Alltsedan uppfinningen av världens första transistor år 1947, har transistorer som är tillverkade av inorganiska halvledarmaterial (som kisel) dominerat den elektroniska industrin. Med tiden har tillverkningsmetoderna för moderna komponenter blivit alltmer komplexa, vilken i sin tur resulterat i högre produktionskostnader. Vid sidan om den höga kostnaden, som är begränsande för en rad elektroniska applikationer, begränsas inorganiska halvledare även av sin mekaniska inflexibilitet och kan inte användas i tillämpningar som kräver flexibla substrat.

Idag, sedan organiska halvledare och ledare har blivit tillgängliga, har nya inriktningar för elektroniska system blivit möjliga. Elektroniska komponenter som tidigare varit olämpliga i vissa tillämpningar, till exempel matindustrin, är nu möjliga att anpassa till nästan varje produkt. Till exempel kan de produceras på plastsubstrat eller appliceras direkt på förpackningar. Jämfört med kiselbaserade komponenter har organiska komponenter en lovande framtid trots sin lägre prestanda, tack vare flera unika egenskaper hos organiska material. För det första kan många av dem beredas från lösningar och kräver inte höga renhetsnivåer. Detta gör det möjligt att producera komponenter via sedvanliga tryckmetoder, vilket möjliggör applikationer med stora ytor, i höga volymer och till låga kostnader. Som en jämförelse tar det vanligen veckor av arbete och kräver ultraren arbetsmiljö att bygga ett kiselchip. Organiska komponenter kan produceras snabbare under mindre noga kontrollerade villkor. För det andra kan organiska komponenter vid tillverkningen samtidigt integreras med andra tillämpningar, t.ex. en organisk sensor invävd i textil. För det tredje är de flexibla och lätta. Eftersom komponenterna är gjorda av tunna filmer, blir de lättviktiga. Man kan göra en elektronisk tidning som väger en femtedel av en vanlig tidnings normalvikt, eftersom det räcker med ett enstaka ark. Tack

vare dessa egenskaper förväntas den organiska elektronikindustrin på sikt bli lika stor som dagens kiselindustri.

Tidiga tillämpningar för ledande polymerer var antistatiska beläggningar, lättviktsbatterier och kretskortsmaterial. Idag har några typer av organiska komponenter börjat röra sig från FoU och laboratorium mot marknaden, och inom de närmaste åren förväntas billiga och även engångs organiska komponenter att dyka upp. Redan nu finns det displayer på marknaden som använder organiska lysdioder. Ett annat exempel är en organisk display. Till skillnad från traditionella displayer kan en organisk display rullas, vilket möjliggör för t.ex. mobila komponenter att ha en display som är större än själva komponenten. Det bör noteras att organisk elektronik förmodligen inte kommer att uppnå samma snabbhet och miniatyrisering som den konventionella elektroniken, men istället kommer den att komplettera och nå till platser som konventionell elektronik inte kan nå.

Den här avhandlingen behandlar organiska komponenter vars funktionalitet involverar elektrolyter. Efter en inledande beskrivning av egenskaperna hos konjugerade polymerer, följer en grundläggande presentation om elektrolyter (jonledningsförmåga, typer, elektriska dubbellagret). Därefter ges en kort översikt över organiska fälteffekttransistorer och även en beskrivning av transistorer som styrs via en elektrolyt.

Acknowledgements

I would never have made it without all the good laughs and all the help and support from family and colleagues. Therefore I would like to express my sincere gratitude to the people who contributed to the completion of this work, and especially to;

Professor Magnus Berggren my supervisor. Thank you for giving me the opportunity to work and study at one of the most outstanding research areas and environments as well as for your help and support during these years.

Associate Professor Xavier Crispin my co-supervisor. Thank you Xavier who always had time for me when I needed help and for your patience, support and encouragement. Thanks for all the help with this thesis.

Docent Nate Robinson, for your all guidance and support, and for all time you have spent helping me and answering my questions.

Sophie Lindesvik, for all the administrational help.

The people that I have worked with, especially the co-authors of the included papers. **Professor Stan Miklavcic** in guidance of my first work at ITN, **Dr. George Baravdish** for giving me the opportunity and helping me teaching, **Mari Stadig-Degerman** for all the fun we had in the preparation and teaching Kemi A for Basåret.

All the present and past members of the **Organic Electronics** research group at ITN (Daniel, David, Edwin, Elin, Emilien, Fredrik, Georgios, Hiam,

Isak, Jiang, Joakim, Klas, Kristin, Lars, Linda, Magnus, Maria, Max, Nate, Olga, Oscar, Payman, PeO, Peter, Sophie, Xavier, Xiangjun and Yu) for many valuable discussions, great friendship and after-work leisure activities.

The personal at **ACREO Norrköping** for all help I got in the lab.

My colleagues and friends; **Frédéric Cortat**, **Allan Huynh**, **Mattias Andersson, Mahiar Hamedi** and **Henry Behnam** for all the fun and discussions in various subjects, as well as for your friendship.

My brothers; **Maurice** and **Robert**, and my sister with family; **Lilian**, **Senharib**, little **David** and **Romi**, for their love, joy and support.

Finally, I would like to thank my dear father and mother; **David** and **Sara**, for their love, for all the support and for always being there.

Elias Said, Norrköping, November 2008

List of Included Papers

Paper I:

Visualizing the electric field in electrolytes using electrochromism from a conjugated polymer

Elias Said, Nathaniel D. Robinson, David Nilsson, Per-Olof Svensson, Magnus Berggren

Electrochemical and Solid-State Letters, **8** (2) H12 - H16 (2005)

Contribution: All the experimental work except the theoretical result. Wrote the first draft and was involved in the final editing of the paper.

Paper II:

Electrostatic potential and double layer force in a semiconductor-electrolyte-semiconductor heterojunction

Stan J. Miklavcic and Elias Said

Physical Review E, **74**, 061606 (2006)

Contribution: Derivation of the electrostatic potential (together with S. Miklavcic) and was involved in the final editing of the paper.

Paper III:

Polymer field-effect transistor gated via a poly(styrenesulfonic acid) thin film

Elias Said, Xavier Crispin, Lars Herlogsson, Sami Elhag, Nathaniel D. Robinson and Magnus Berggren

Applied Physics Letters, **89**, 143507 (2006)

Contribution: All the experimental work. Wrote the first draft and was involved in the final editing of the paper.

Paper IV:

Effects of the ionic currents in electrolyte-gated organic field-effect transistors

Elias Said, Oscar Larsson, Magnus Berggren and Xavier Crispin

Advanced Functional Materials, **18**, 3529 - 3536 (2008)

Contribution: All the experimental work. Wrote the first draft and was involved in the final editing of the paper.

Paper V:

Electrochromic display cells driven by an electrolyte-gated organic field-effect transistor

Elias Said, Peter Andersson, Isak Engquist, Xavier Crispin and Magnus Berggren

Submitted

Contribution: All the experimental work. Wrote the first draft and was involved in the final editing of the paper.

Table of Contents

1 Introduction to Organic Electronics

Since the discovery of the world's first transistor in 1947, thin-film transistors made of inorganic semiconductor materials, such as silicon, have come to dominate the electronic industry. Nowadays the processing methods for fabricating devices become increasingly more complex, resulting in higher production costs. Beside the high cost that limits the range of applications in daily life, poor mechanical flexibility also limits use in applications requiring flexible substrates.

When organic semiconductors and conductors became available, new routes for electronic systems were opened. Electronic devices that were previously thought to be unsuitable in some applications, such as in the food industry, are now brought closer to nearly every product. For instance, devices can be produced on plastic substrates and applied on packages. Compared to silicon based components, organic-based electronic devices have a promising future despite their lower performance as semiconductors because of several unique properties of organic materials. First, many of them can be processed from solution and do not require high purity levels. This makes it possible to produce components using conventional printing techniques, which allow large area, high volume and low-cost applications. In comparison, building a silicon chip usually takes weeks of work and requires an ultra clean working environment. Organic devices can be faster produced under less carefully controlled conditions. Second, organic devices can be made and integrated together with other applications simultaneously, for example an organic sensor device woven into textiles. Third, they are flexible and, because the devices are based on thin films, they are lightweight. An example of the benefits of weight reduction is the replacement of conventional newspapers

with electronic ones: up to an 80% reduction of paper would be used[1]. Thanks to these features, the organic electronic industry is expected to become as big as the silicon industry and will have a large impact on our daily life. However, we always have to be aware that organic electronics alone are not going to make it.

Figure 1. A mobile device rollable polymer display for reading personal information, newspapers and books (by Polymervision, www.polymervision.com). The display type is based on rollable organic thin-film transistor backplane with electrophoretic front plane with a total thickness of about 0.1 mm, equal to the thickness of everyday paper.

Some of the earliest applications of conductive polymers were the production of antistatic coatings, lightweight batteries and materials for circuit boards. Today, organic (opto)electronic devices are beginning to move beyond R&D and into the market, such that in the next couple of years low-cost and even disposable organic electronic devices will emerge. Already, displays that use organic light-emitting diodes (OLEDs) are found on the market. Another example of polymer displays that have entered the market is shown in figure 1. Unlike conventional displays, polymer displays can be rollable, which enables for instance mobile devices to incorporate a display that is larger than the device itself. It should be noted that organic electronics may never match the switching speed and miniaturization of conventional electronics but they will compete and go to places that the conventional semiconducting industry cannot reach.

This thesis deals with organic-based devices whose working mechanism involves electrolytes. After describing the properties of conjugated polymers in chapter 3, fundamentals on electrolytes (ionic conductivity, types and electric double layer) are briefly presented in chapter 4. Chapter 5 gives a short review of the field of organic field-effect transistors as well as a description of transistors that are gated via an electrolyte.

2 The Motivation

Most electronic components and systems are built on substrates such as silicon wafers and glass, resulting in electronics that are fragile and have a lack of both conformability and flexibility. Organic semiconductors offer the possibility of producing flexible electronic devices using conventional printing techniques. Because of the technological potential of this class of semiconductors, chemists, physicists and engineers are working hand in hand to improve:

- Firstly, the performance of organic (opto)electronic devices. The power consumption of organic-based device and their compatibility with power sources, like batteries, is an important feature when targeting portable electronics. Hence, many efforts are devoted to finding alternative routes to lower the operating voltage of organic electronics.

- Secondly, the manufacturing process of the devices. Organic electronic devices are expected to show up in low-cost products (single use) because of their solution processibility. Indeed, thin films of organic semiconductors can be fabricated via printing techniques. While hundred nanometer thick films can be formed by ink-jet printing, other printing techniques more adapted to reel-to-reel applications commonly use micrometer thick layers. Hence, a challenge to be able to use low-cost manufacturing technique is to find new materials and new device concepts compatible with thicker films.

An example illustrating an approach combining low operating voltage and a thick active layer is found in organic light-emitting devices. In organic light-emitting diodes (OLEDs)[2], the organic semiconductor layer is sandwiched between two electrodes. The use of a high work function anode and a low work function cathode ensure rectification and efficient electron and hole injection in forward bias. The recombination of the charge carriers generates photons: this is electroluminescence. While those devices are on the market in various displays, none of their manufacturing step uses a reel-to-reel process for two reasons: (i) OLEDs require thin organic films (hundreds nm) to keep the operating voltage low (~10 V); (ii) the deposition of low work function (air reactive) metals is not compatible with reel-to-reel technology. Researchers have found interesting features by combining organic semiconductors with electrolytes. In the case of light emissive devices, the organic light-emitting electrochemical cell (OLEC)[3] was developed 13 years ago. In contrast to OLEDs, the emission layer in OLECs consists of a light-emitting polymer which is blended with a solid electrolyte that contains ions creating a mixed conductor, which transports both electrons and ions in a single composite film. Upon applying a bias of a few volts (voltage equal or greater than the polymer band gap), electric double layers are formed at each electrode/active layer allowing efficient charge injection independently of the electrode work function. In OLECs, there is no need of a low work function metal to inject electrons. The injected electrons and holes attract compensating cations and anions in n-type and p-type doping. When the doped regions get close to each other, a p-i-n junction is formed. Electrons are injected from the n-doped side to the undoped semiconductor region in the middle; while holes are injected from the p-doped side into the undoped semiconductor region. The resulting electron-hole recombination in the undoped semiconductor region gives rise to light emission. Compared to OLEDs, OLECs operate at low voltages (< 4 V), which in combination with a high electroluminescence quantum efficiency results in high power efficiency. Moreover, the low voltage operation remains whatever the thickness of the active layer since the double layers, formed spontaneously at the metal-semiconductor interfaces, govern the charge injection.

In this thesis, we aim to explore the richness of the combination between semiconductors and electrolytes. Our strategy has been to classify the various electrolyte-semiconductor systems, understand them, and then use those to introduce new functionality in organic electronic devices. The polarization of a semiconductor-electrolyte system gives rise to the creation of electric double layers, also called Helmholtz double layers, with a layer of ions in the electrolyte and a layer of electrons (holes) in the semiconductor. At that stage, the ions can or cannot penetrate into the semiconductor depending on the chemical nature of the ions and the chemical nature of the semiconductor. For semiconductors with high cohesive energy (covalent bonds) like inorganic semiconductors (e.g. silicon), the molecular ions cannot penetrate into the bulk semiconductor and the electrolyte-semiconductor interface is composed of the electric double layer. For organic semiconductors with lower cohesive energy (Van der Waals interactions), ions can easily penetrate into the bulk and thus propagate the electrochemical reaction starting from the interface into the bulk of the semiconductor.

Secondly, we want to find materials that allow the formation of an electrolyte-organic semiconductor interface without penetration of ions into the organic semiconductor (i.e. without bulk electrochemical doping). Such an electrolyte-organic semiconductor system can be used as the insulator-semiconductor interface in a field-effect transistor. Unlike dielectrics that polarize upon applying a negative voltage to the gate (left hand side in figure 2), the cations in the electrolyte migrate towards the negatively charged gate forming an electric double layer (EDL) at the electrolyte/electrode interface, while the remaining anions stay close to the organic semiconductor allowing the formation of the channel (right hand side in figure 2). This new type of transistor can be called an Electric Double Layer Capacitor gated Organic Field-Effect Transistor (EDLC-OFET). The small distance (~1 nm) between the charges at the electrolyte/organic semiconductor interface gives rise to

large capacitance of the EDLC (~10 μF/cm²) resulting in a remarkable reduction of the operation voltage compared to traditional OFETs. Importantly, this high capacitance is, in principle, not dependent on the thickness of the electrolyte since the significant distance for the capacitor is the distance between the ion and the semiconductor surface created after ion migration at the electrolyte-semiconductor interface. Hence, thick electrolyte layers can be used, allowing for both the electrolyte and organic semiconductor layers to be printed.

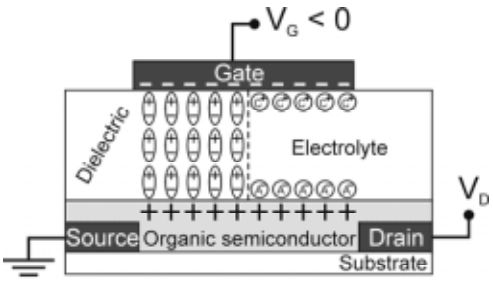

Figure 2. Schematic cross section of an OFET with either a dielectric or an electrolyte as gate insulator. Upon applying a negative gate voltage V_G, the dielectric material will polarize and electric dipoles are created. Cations (C^+) will migrate towards the gate and form an EDL at the interface between the electrolyte and the electrode, while the anions (A^-) will be migrating at the electrolyte/semiconductor interface, thus inducing the formation of a positively charged channel between source and drain.

3 Polymers: From Insulators to Conductors

3.1 Electronic structure of conjugated polymers

Polymers that are assigned as conventional polymers, also called plastics, have been considered for a long time as insulators. At the beginning, polymers were used in clothes, tools, plastic bags, wire shielding and many others applications[4]. A huge interest in polymer science started when important discoveries concerning modification and creation of semi-synthetic polymeric materials as rubber were made from natural polymers. This gave rise later to the development of a large number of fully-synthetic polymers, such as polystyrene and poly(methyl methacrylate). Polymers are macromolecules that are formed by linking together monomers in a chain through a chemical reaction known as polymerization[5]. The formed polymer chains can have linear, branched or a network structure.

The main element in many polymers is the carbon atom C. The valence electron configuration for a C atom is $2s^2 2p^2$ or $2s^2 2p_x^1 2p_y^1$. With this configuration, the C atom can form two bonds and not four with other atoms. In early models, the chemical structure of methane has been explained as follows: Forming four bonds would require that one 2s electron is excited to an orbital with higher energy leading to the configuration $2s^1 2p_x^1 2p_y^1 p_z^1$. This process is called promotion[6]. The unpaired electrons in separate orbitals of the promoted C atom can be paired with four 1s electrons of hydrogen and form a methane molecule. It must be noticed that excitation of the 2s electron to a higher orbital requires an investment of energy. However, globally the formation of methane is thermodynamically favorable because of the stabilization encountered upon the formation of the four C-H bonds. A similar bonding configuration for the C atoms is found in

a polyethylene chain, which consists of a monomeric repeat unit -(CH_2 – CH_2)$_n$-where each carbon is sp^3 hybridized. Each C atom binds to other four adjacent atoms by sigma (σ) bond (figure 3.1a). The wave function of the σ-electrons are formed by the large overlap between the sp^3 hybrid atomic orbitals, which in turns form wide σ-bands, but also large band gap between the σ-band and the σ*-band. For polyethylene, the optical band gap is on the order of 8 eV[7]. The high band gap makes conventional polymers electrical insulators and transparent.

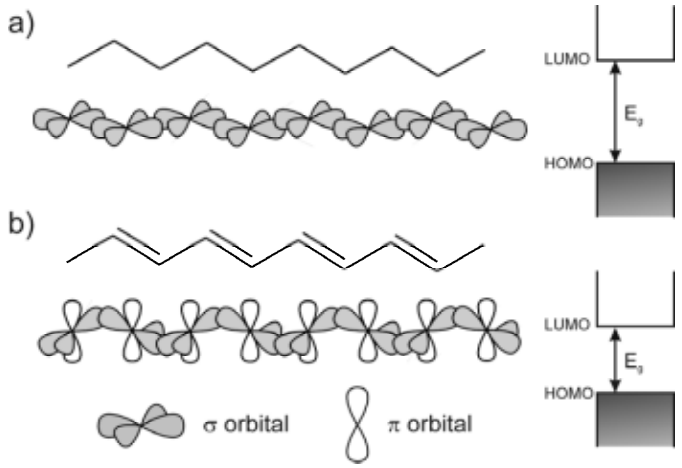

Figure 3.1. A schematic representation of the structure and atomic orbitals involved in the electronic structure (left) and the energy diagram (right) of a) polyethylene, b) trans-polyacetylene. In polyethylene each carbon atom forms four σ bonds with other atoms (2 carbon and 2 hydrogen atoms), whereas in case of polyacetylene three σ bonds and one π bond are formed, resulting in alternating single and double bonds. The difference between HOMO and LUMO defines the band gap E_g of the neutral polymer chain. For conventional polymers E_g is greater than 5 eV.

There exists another class of polymers with quite different properties, called conjugated polymers. The simplest conjugated polymer that has been extensively studied is trans-polyacetylene (figure 3.1b). Unlike conventional polymers formed entirely by σ bonds, in conjugated polymers, each C atom forms three σ bonds with other atoms in the sp^2 hybridized state. The

remaining electrons in the p_z orbital of adjacent carbon atoms overlap with each other to form delocalized π-orbitals forming π-bands. Since there is one electron per p_z orbital and there is the same numbers of π-orbitals than there are p_z orbitals involved, conjugated polymers with equal bond lengths would have half-filled band like metals, but this is not the case. The reason is the Peierls instability that states that a one-dimensional metal is unstable and will undergo structure distortion opening a band gap and becoming a semiconductor. The structure distortion results in alternating single and double bonds. Therefore there is a filled valence band and an empty conduction band. The top of the valence band is called the highest occupied molecular orbital, HOMO; and the bottom of the conduction band is called the lowest unoccupied molecular orbital, LUMO. The energy difference between these two states defines the energy band gap E_g, which is in the range of visible light and near infrared (4 eV to 1 eV), similar to inorganic semiconductors. In other words, pure conjugated polymers are semiconductors.

3.2 Electrical properties of conjugated polymers

To increase the conductivity of the conjugated polymers, doping of these materials is necessary. Doping can be obtained chemically via a redox reaction with a dopant molecule or electrochemically by charge transfer with an electrode. The first high conducting polyacetylene was achieved via chemical doping when a film of polymer was exposed to iodine vapor. Figure 3.2 illustrates the conductivity range for polyacetylene[8] and other conjugated polymers compared with other common materials. In electrochemical doping, the doping level is determined by the applied voltage between the conducting polymer and the counter electrode. The doping charge is supplied by the electrode to the polymer; while oppositely charged ions migrate from the electrolyte to balance the electronic doping charge. This resembles an electrochemical cell. Doping is reversible (if not kinetically blocked). The electrochemical doping of the π-polymer is illustrated by the following formulas:

$(\pi\text{-polymer})_n + [M^+X^-]_{solution} \rightarrow [(\pi\text{-polymer})^{+y}(X^-)_y]_n + [M]_{electrode}$ (p-type doping)

$(\pi\text{-polymer})_n + [M]_{electrode} \rightarrow [(M^+)_y(\pi\text{-polymer})^{-y}]_n + [M^+X^-]_{solution}$ (n-type doping)

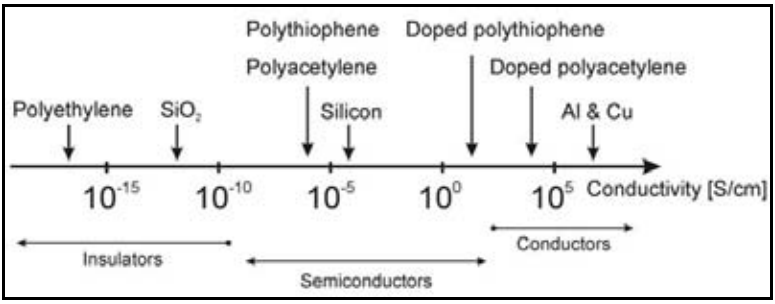

Figure 3.2. Electrical conductivities of conjugated polymers compared with other common materials.

Generally, charge carriers in conventional semiconductors are created by addition or removal of electrons (or by photoexcitation). These charge carriers (electrons and holes) are delocalized in the crystal structure. In conjugated polymers the nature of charge carriers is different. Electrons or holes will not be generated at HOMO or LUMO upon addition or removal of electrons from the polymer, instead a defect, which is associated to a molecular distortion in the polymer chain, is created. Unlike conventional semiconductors, this defect is localized on the polymer chain and results in specific energy levels in the electronic structure of conjugated polymers. These defects include the quasi-particles solitons, polarons and bipolarons. Solitons as charge carrier species exist in polymers with a degenerate ground state system formed by two geometries of polymer units with the same energy (change of bond length alternation). A polymer with a degenerate system is trans-polyacetylene. Solitons originate from the odd number of carbon atoms in trans-polyacetylene chains. The soliton is an unpaired electron located at the border line between two phases with different bond

length alternations. This unpaired electron is lying to an energy level in the middle of the band gap of the polymers (figure 3.3a). The unpaired electron in the state leads to a neutral soliton with spin ½. Unoccupied or doubly occupied, the state of the soliton is charged and spinless. The soliton is mobile along the polymer backbone. When doping levels become high enough, the charged solitons start to interact with each other forming a soliton bands (figure 3.3b). These bands will eventually merge with the edges of HOMO and LUMO to create metallic conductivity[9,10].

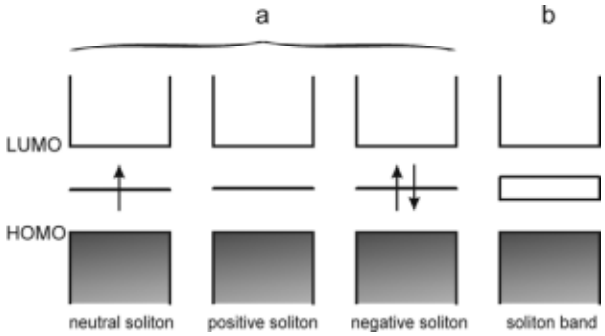

Figure 3.3. a) The oxidation and reduction of the neutral soliton (left) results in positive (center) and negative (right) soliton. b) High redox-doping forms soliton band.

Most of conjugated polymer systems are non-degenerate ground state systems. In these polymers the interchange of the single and double bonds produces higher energy geometric configuration. Addition or removal of an electron on a neutral segment causes distortion and formation of a localized defect that moves together with the charge. This combination of an additional charge coupled to local lattice distortion is called a polaron[11]. Depending on the sign of the charge remove, one speaks about positive polarons or negative polarons. The polaron has a localized electronic state in the band gap (figure 3.4a). Upon further addition of charges to the polymer chain, two charges might couple together, despite electrostatic repulsion, thanks to lattice distortion to create bipolarons (figure 3.4b). At high enough doping level a bipolaron band is formed and eventually merges with the HOMO and LUMO bands respectively to produce partially filled bands and

metallic like conductivity (figure 3.4c). Unlike polarons, bipolarons are always charged and have zero spin.

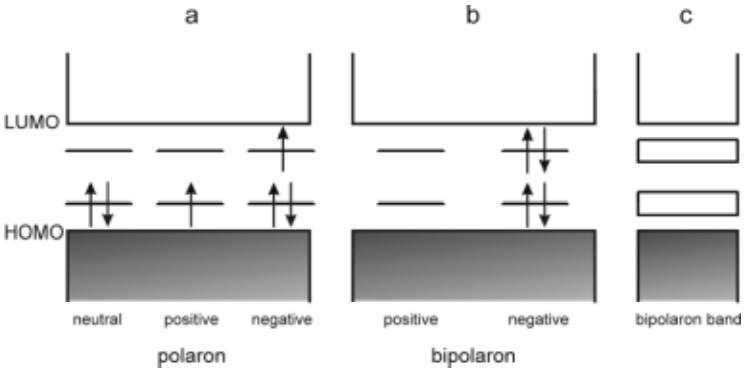

Figure 3.4. The energy diagram of a polymer with a non-degenerate ground state system. Upon doping new localized states are created. a) The oxidation and reduction of the neutral polaron (left) results in positive (center) and negative (right) polaron. b) When two polarons bind together a bipolaron will be formed. Neutral bipolaron does not exist. c) High redox-doping forms bipolaron bands.

Conduction processes are related to the mobility and the density of charge carriers. For band-like transport, charge carriers occupy delocalized states. This kind of transport is typical for crystalline semiconductors and metals. In conducting polymers however, the transport is dominated by variable range hopping or tunneling processes[12,13]. The charge carriers are transported through hopping between localized states in the band gap. Note that the disorder in the material will influence and even limit the charge transport. Well-ordered polymer films have usually better charge transport properties. The hopping process requires energy provided by the phonons. Therefore the hopping conductivity increases with the temperature, contrary to band-like conductivity, and is finite at zero temperature. Charges are transported via interchain hops between π-orbitals of adjacent chains. In doped conjugated polymers, the transfer of the charge can be affected by the intermediate doping ions. Upon high doping, the charge transport of the conjugated polymers is based on metallic grains surrounded by a media with

localized states in the band gap[14]. In the grains the transport is band-like because the polymer chains are densely packed, whereas between the grains the charge transport will be limited to hopping or tunneling mechanism.

3.3 Optical properties and electrochromism

The electronic structure of the conjugated polymers is not only important in the description of the electrical properties, but it also determines their optical properties. Because the band gap of the conjugated polymers lies between 1 eV to 3 eV, the materials can therefore absorb light from the near infra red, the visible to the UV region. In order to absorb light, the energy of the photons must be equal to the band gap energy. Upon absorption, the electronic system increases its energy. This complex phenomenon can be regarded in a first approximation as the promotion of an electron from an occupied to a higher empty energy state. The transition to the first excited state thus corresponds to the HOMO to LUMO transition. The resulting hole in HOMO and electron in LUMO represents an electron-hole pair also called exciton. Since the excited electron that is created by the absorption is out of balance with their environment, it returns back or relaxes to its ground state. Relaxation of the electron results in either emitting the energy as radiation or through non-radiative processes. The energy of the emitted light is always lower than the absorbed light energy because some of the energy is lost in vibrational relaxations. The absorption and emission processes are illustrated in figure 3.5a.

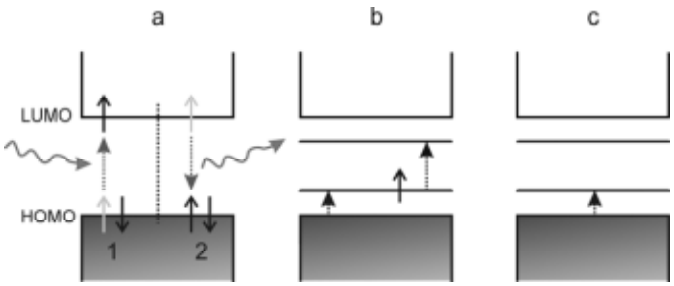

Figure 3.5. a) Absorption and emission processes. In absorption (1) the electron is excited due to absorption of the photon energy. A photon is emitted (2) when the electron is relaxed back to lower energy state. Optical transitions in positive b) polaron and c) bipolaron doped case for polythiophenes. The new states in the band gap give other possible transitions compared to the optical transitions in the neutral state (1) in a, two possible transitions in the polaron case while one is observed under bipolaron doping.

Upon positive or negative doping (removal or addition of electrons) of the conjugated polymer chains, new polaronic or bipolaronic levels appear in the band gap of the neutral polymer, as previously described. As a consequence, doped systems have new optical transitions to and from these levels (see figure 3.5b and c). When the doping is realized via electrochemistry, the accompanied change of optical band gap is called electrochromism[15-17]. Electrochromism can easily be demonstrated in an electrochemical cell with two polymer electrodes connected via an electrolyte, a typical display element structure (figure 3.6). Upon application of an appropriate potential between the electrodes, the negatively biased polymer electrode is reduced while the other oxidizes, causing a color change in one or both of the electrodes. This doping/de-doping redox switch is fully reversible and can be repeated many times[18].

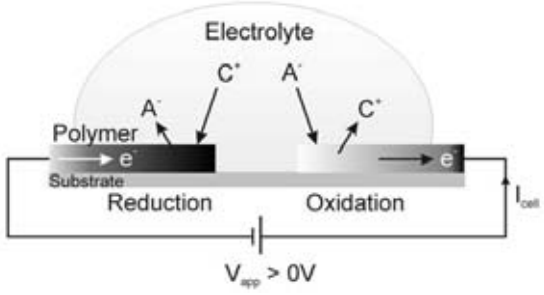

Figure 3.6. Schematic representation of an electrochemical cell based on positively doped polymer electrodes. When a voltage is applied the positively biased polymer one electrode is oxidized while the other reduces. At the oxidized polymer electrode, the concentration of positive (bi)polarons is increased, therefore anions A^- (or cations C^-) migrate into (out) the polymer film in order to maintain the electroneutrality. On the contrary, the reduced electrode

undergoes a decrease of a positive polaron and the migration of oppositely charged ions from the electrolyte. This type of cell is typically used as a display element.

Doping of the conjugated polymers causes an increase of electronic conductivity and a color change. This feature makes conjugated polymers useful in many applications such as displays[19], smart windows[20] and in determining the direction and the magnitude of the electric field in electrolytes[21]. The color change between doped and undoped forms of the polymer depends on the magnitude of the band gap of the undoped polymer. Thin films of polymers with band gaps greater than 3 eV are colorless and transparent in undoped form, but colored in the doped state. Conversely, for band gaps in order to or less than 1.5 eV, polymer films are colored in undoped state and transparent in doped state, since the polaronic states create optical absorption in the infra-red region. Polymers with intermediate band gaps, as polypyrrole, will switch between yellow-green (insulating) to blue-violet (conductive) upon reversible oxidation[11].

3.4 Examples of specific conjugated materials

3.4.1 Poly(3,4-ethylenedioxythiophene)

Poly(3,4-ethylenedioxythiophene), abbreviated as PEDOT, is one of the most successful conducting polymers, which was developed by the scientists at the Bayer AG research laboratories in Germany[22]. PEDOT is synthesized by chemical or electrochemical polymerization of EDOT monomers in an aqueous solution comprising the electrolyte. The positive doping charges carried by PEDOT are balanced by the counter anion poly(styrenesulfonic) (PSS^-). The resulting polymer blend PEDOT:PSS has been intensively investigated and used in different research applications (figure 3.7). In the work presented in paper I, thin film of PEDOT:PSS, 200 nm thick (named Orgacon™ foil[23]) on plastic substrate has been used.

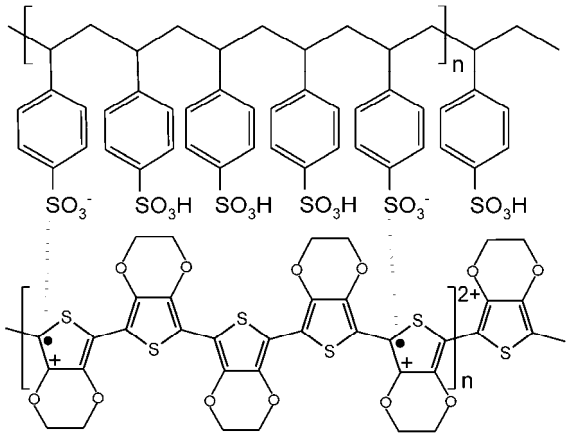

Figure 3.7. The chemical structure of poly(3,4-ethylenedioxythiophene), PEDOT (lower part of the figure) with poly(styrene sulfonic) acid, PSS^-, as counterion (upper part). The positive bipolaron responsible for the charge transport in PEDOT:PSS is also sketched.

Neutral PEDOT has a band gap of 1.6 – 1.7 eV that makes it having a deep blue color. The band gap can be controlled by using various oxidative agents giving rise to neutral polymers with colors ranging over entire rainbow of colors[22]. Because of its low oxidation potential, films of neutral PEDOT are not stable and oxidize rapidly in air. Therefore handling under an inert atmosphere is required. In the doped and conducting (oxidized) state, PEDOT:PSS films with conductivities between 1 and 10 S/cm are highly stable and have high transparency in the visible region (strong near infrared absorption)[24]. The reduction formula of the doped PEDOT is represented by the half reaction

$$PEDOT^+ : PSS^- + M^+ + e^- \quad \rightarrow \quad PEDOT^0 + M^+ : PSS^-$$

where M^+ denotes a positively charged ion and e^- an electron. The reduction to the neutral state results in a decrease in the number of charge carriers in PEDOT, giving rise to a decrease in conductivity[25] and a shift of the optical absorption spectrum from the near infrared region into the visible region. The positive charge in doped PEDOT is delocalized over several monomer

units[22]. Thus, the representation $PEDOT^+$ in the above equation is intended to represent a group of consecutive monomer units.

The electrical conductivity of PEDOT can be enhanced through morphology change. For example, conductivity of PEDOT:PSS has been increased three orders of magnitude when a secondary dopant diethylene glycol (DEG) was added to the PEDOT:PSS emulsion[26]. The origin of the high conductivity is attributed to the phase separation of the excess PSS from the PEDOT:PSS regions which results in better pathways for conduction and an interconnected three dimensional conducting network.

PEDOT:PSS was initially developed for antistatic applications in the photographic industry[23], but it took no long time to find the use of this conducting polymer in other applications. Thanks to its high stability and conductivity, easy processibility and even the electrochromic properties, PEDOT:PSS is one of the promising candidates for developments in the area of the cheap and flexible electronic systems. It can now be found as the electrode or conductor material in electrochemical transistors[27], organic field-effect transistors[28], organic light-emitting diodes[29], electrochemical displays[19], smart windows[20], batteries and capacitors[30,31].

3.4.2 Poly(3-hexylthiophene)

Polythiophene and its derivative, the poly(3-hexylthiophene) (P3HT) is one of the most studied semiconducting polymer due to its high hole mobility, good solubility and processability[32]. It is stable both in doped and undoped state. The 3-hexyl substituent in a thiophene ring can be incorporated into a polymer chain with two different regio-regularities[33], shown in figure 3.8a: head to tail (HT) and head to head (HH). A regio-random P3HT consists of both HH and HT 3-hexylthiophene in a random pattern, while a regio-regular P3HT (figure 3.8b) has only one kind of 3-hexylthiophene. Regio-regular P3HT has great potential as organic semiconductor in organic electronics

because of its strong tendency to self-assemble into crystallites with ordered structures upon casting into thin films, giving thus rise to carrier mobilities in order of 0.1 $cm^2 V^{-1}s^{-1}$[34]. On the contrary, the regio-random P3HT has a twisted chain conformation with poor packing and low crystallinity, resulting in mobilities of only 10^{-4} $cm^2 V^{-1}s^{-1}$[33] and in a higher optical band gap than its regio-regular structure. Depending on processing conditions and regio-regularity of the polymer, the polymer chains can be ordered in two different orientations, parallel and normal to the substrate[34]. With electrodes in the plane of the substrate, researchers showed that the transport in regio-regular P3HT is highly anisotropic. The mobility has been found to be three orders of magnitude higher when π-stacking direction is parallel to the direction of charge transport, thus demonstrating fast and efficient interchain transport of the carriers. The morphology and charge transport of the regio-regular P3HT has also been shown to depend on the molecular weight (MW)[35]. In addition, the choice of solvents strongly influence the microscopic morphology of the film and thus its mobility[32].

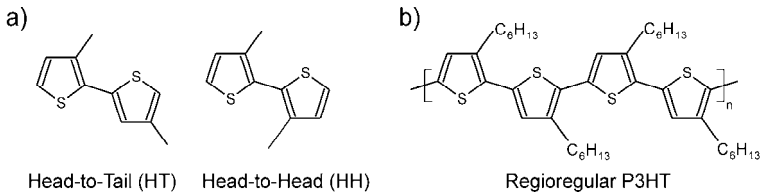

Figure 3.8. a) Two different regioregularities that can be incorporated into a polymer chain. b) The chemical representation of regio-regular poly(3 hexylthiophene) (P3HT).

3.4.3 Polyaniline

Polyaniline, PANI, is another popular conjugated polymer[36,37]. Thin film of PANI exhibits multiple colors depending on the redox state (figure 3.9). The electrical and electrochromic properties of PANI do not only depend on the oxidation state but also on the protonation state, as shown in figure 3.9a. Hence conductivity can be tuned simply by changing the pH value of the electrolyte. It can exist as salts or bases in three separate oxidation states.

The neutralized thin film of PANI is transparent yellow and insulating (leucoemeraldine). Upon oxidation in acidic medium, the film turns green and becomes conducting (emeraldine). Further oxidation gives rise to a blue color that is characteristic of the pernigraniline form. When the conductive emeraldine PANI, which is protonated, comes in contact with a base solution, it deprotonates and becomes blue emeraldine base (figure 3.9b), which is an insulator. The protonation and deprotonation processes is reversible. To get back the conductive PANI, the film should be immersed in an acid solution. The resistivity of well ordered PANI film decreases when the temperature is lowered down to 5 K, indicating the metallic behaviour of the film[38]. This polymer has found applications as a stable and low-cost conductor[39], in electrochromic display window[17], as electrodes in organic transistors[40], as ion and pH sensors[41] and in battery materials[42].

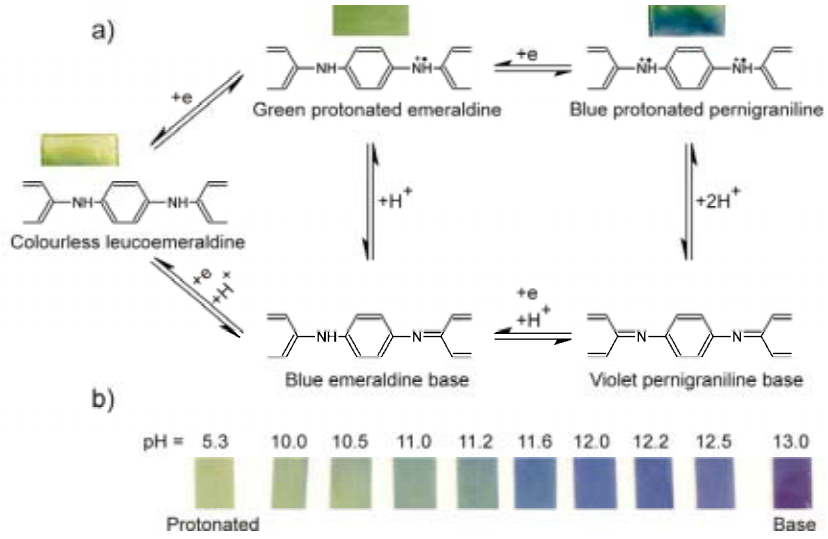

Figure 3.9. a) The redox and protonation states of PANI. The inserted images are showing the multi electrochromism properties of green protonated emeraldine film when it became oxidized (pernigraniline) and reduced (leucoemeraldine). Notice that the PANI film was in contact with a gelled electrolyte that in turn was connected to the outer electrodes. b) Deprotonation of emeraldine film when immersing it in a solution with different pH. The contrast of the blue color is strong at high pH levels.

4 Electrolytes

Any substance containing mobile ions, which give rise to electrical conductivity, can be deemed an electrolyte. Electrolytes can be found in liquid phase, but also in molten or solid form. Depending on the concentration of mobile ions (i.e. solute), the ionic conductivity can vary drastically. Depending on the solute dissociation that forms free ions, electrolytes are usually divided into two classes, strong and weak. In strong electrolyte (e.g., salts or strong acids), all or much of the solute is dissociated and the ionic conductivity is quasi constant with the solute concentration. If the solute is partially dissociated in aqueous solution, the ionic conductivity depends strongly on the solute concentration and this is called a weak electrolyte (e.g., weak acids and bases). In addition, the choice of the solvent should be considered in electrochemical applications. Each solvent has a defined potential window within which it is stable and beyond which it can decompose. The use of non-aqueous electrolytes for electrochemical applications is often preferred due to a wider stability potential window, which allows using higher operating voltages[43]. For example, water has a narrower potential window (~2 V) than acetonitrile (~4.5 V), which makes it unsuitable for electrochemical measurements that require higher potentials.

4.1 Solid electrolytes

Solid electrolytes, also known as fast ionic conductors, are, in contrast to liquid electrolytes, electrolytes that do not need a solvent for the ion motion. Solid electrolytes have usually one component of the structure, cationic or anionic, which is essentially free to move throughout the bulk. The advantages of using solid electrolytes in practical applications are many. The chemical and electrochemical stability and the flexibility of the material

makes it mechanically robust; thin films are easily processed on large areas. Solid electrolytes have a wide range of applications, for instance in batteries[44] and electrochemical capacitors[45], electrochromic devices such as smart windows[46] and in fuel cells[47]. Some solid electrolytes are polymer based, which include two general categories: polymer electrolytes and polyelectrolytes.

4.1.1 Polymer electrolytes

Polymer electrolytes are composed of a salt dispersed in a neutral polymer matrix (that is not itself an electrolyte)[48]. The salt is dissociated into ions screened by the polymer matrix. The ion motion is coupled to local motion of the polymer chain and transition between ion coordinating sites[48]. The most studied polymer electrolytes are poly(ethylene oxide) (PEO) (figure 4.1a) that consists of the repeating units of ether groups $(-CH_2CH_2O-)_n$[48,49] and the lower molecular weight polymer poly(ethylene glycol) (PEG)[50,51]. PEO is still one of the useful candidates in designing new types of batteries[52]. PEO exhibits low ionic conductivity (10^{-9} - 10^{-8} S cm^{-1}) at room temperature because of its tendency to crystallize. Depending on the molecular weight, the melting point of PEO varies from 46 °C for low weight (200 kDa) to 60 °C for high weight (4 MDa)[53]. Thanks to the ability to dissolve high concentration of salts such as lithium and sodium salts, the crystalline phase is suppressed, enhancing the amorphous phase that results in higher ionic conductivity[54]. In addition, PEO is soluble in water and a number of common organic solvents.

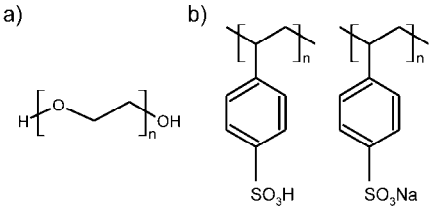

Figure 4.1. a) The ether group repeating unit of poly(ethylene oxide) (PEO). b) Poly(styrenesulfonate) (PSS^-) with labile H^+ (left) and Na^+ (right) as cations, while the anions are the sulfonate pendant groups attached to the polymer chains.

4.1.2 Polyelectrolytes

Polyelectrolytes are polymers that bear ionized units[55]. The small mobile counter ions in polyelectrolyte aqueous solutions dissociate making the immobile polymer chains charged. The conductivity of aqueous polyelectrolyte solutions is on the order of 100 μS cm^{-1}[56]. The polyelectrolytes presented in figure 4.1b are strong polyelectrolytes in solution in which anions are covalently bonded to the polymer backbone. However, in solid phase, because of the lack of screening solvent, the electrostatic potential attraction between the immobile ions and the charged polymer chain is large and some mobile ions remain bound to the polymer chains. This is known as a counter ion condensation phenomena[55,56] that divides the counter ions into bound and free counter ions. Bound counter ions stay in the vicinity of the charged polymer, while the free ions dissociate from the polymer chain and interact through a screened Coulomb potential[56]. Poly(styrenesulfonate) (PSS^-) either with protons as counter ions or sodium (Na^+) is displayed in figure 4.1b. In polyelectrolytes, the activation energy decreases strongly with increasing the humidity, as the partial solvation of ions with water molecules results in a decrease of activation barrier for the ion transport. Additionally, like for Nafion^R, a fluorinated polysulfonic acid, hydrophilic channels can swallow and improve the ion mobility. To this end, Nafion^R has been used as a material for sensing humidity in an electrochemical transistor[57]. Gelled PSS:Na, prepared by mixing together with other hygroscopic materials, has also been used to achieve higher ionic conductivity in amorphous or semi-solid phase for application in electrochemical devices[19].

4.2 Ionic conductivity and transport

As for all charge transport phenomena, the ionic conductivity in electrolytes depends both on the density and the mobility of the charge carrier. The charge carriers are in this case are ions. The factors that determine the concentration are the solubility and the degree of dissociation[58].

The ionic conductivity, κ, of an electrolyte is given by

$$\kappa = \frac{1}{\text{Resistivity (in } \Omega\text{m)}} \tag{4.1}$$

Because the ionic conductivity depends on the number of conducting ions presented in the electrolyte, it is usually expressed in terms of the molar conductivity, which is defined as the conductivity divided by the concentration,

$$\text{Molar conductivity} = \frac{\text{Conductivity}}{\text{Concentration}} = \frac{\kappa}{c} \tag{4.2}$$

The transport of electricity through electrolytes differs fundamentally from electronic conduction in that the carriers are ions, which possess certain dimensions and masses that are much larger than electrons (or holes). Beside that, similar phenomena are found. When no external field is applied, in presence of a concentration gradient of ions, a diffusion current is created. The presence of an external field results in migration, i.e. an ionic movement parallel to the electric field. So, ionic currents can originate both from diffusion and migration. However, the main difference between these two processes[58] is that, in migration, the positive and negative ions move in opposite direction, while they can eventually move in the same direction in the case of diffusion, depending on the slope of the concentration profile for each specific ion.

The migration of mobile ions in a solvent under an electric field, *E*, depends on the viscosity of the solvent, η, and its charge ze [45]. The limiting speed of the ion is obtained when the frictional force (proportional to the viscosity) equals the electrical force created by the electric field.

$$\frac{\nu}{E} = \frac{ze}{6\pi\eta r_i} \tag{4.3}$$

where ν is the average velocity of the ion under *E*, r_i is the radius of the solvated ion and $\frac{\nu}{E}$ is the mobility of the ion. The equation predicts that the product of $\frac{\nu}{E}$ and η should be constant for the mobility of an ion in various solvents with different viscosities. This relation is referred to Walden's rule[58]. However, taking into account the variation of r_i in various solvent and the relevant η, which is an effective viscosity that applies locally near the ion as it moves, the relation is not always followed. Note that for high ionic concentration, the ion-ion interactions are important and will affect the transport[45].

When the medium surrounding the ions is not composed of small solvent molecules but rather a non-ionic polymer host material, like in polymer electrolytes, the mobility is dependent on the activation energy necessary for ions to jump from one site to the next, rather than by the viscosity of the matrix. The ions are not transported with a shell of solvent molecules in a dry polymer electrolyte. The ionic conductivity of solid electrolytes is usually several orders of magnitude lower than the ionic conductivity of liquid electrolytes, because of a lower mobility and smaller concentration of ions. A too high ion concentration leads to the formation of ionic crystallites in the

matrix. Note that upon annealing, the conductivity increases dramatically at the phase transitions (glass transition and fusion).

In a dry polyelectrolyte, the ion mobility is low and the transport mechanism is similar to the polymer electrolyte. Additionally, the humidity strongly increases the ionic conductivity. In that case, water partially solvates the mobile and polymeric ions, which results in a lower activation energy for the ion hopping.

4.3 Methods to measure the ionic conductivity

Impedance spectroscopy is used extensively as a two-probe technique (figure 4.2a) to study the electronic and electrochemical properties of electrolytes[49,56]. The results that are obtained from impedance spectroscopy can be converted to appropriate equivalent circuits. The parameters of the circuits are then related to the carrier transport properties, i.e. the ionic conductivity, the electrolyte resistance and double layer capacitance. In impedance spectroscopy measurements, a small alternating voltage (ac) is applied with known frequency (*f*) and small amplitude to a sample and an ac current that has same frequency as the voltage but a phase shift is measured. The impedance is defined by Ohm's law and consists of a real and an imaginary part. The real part (Z´, related to a resistance) is plotted versus the imaginary part (Z´´, related to the capacitance) in a so-called "Nyquist impedance plot", to determine the equivalent circuit (figure 4.2b). An ideal Nyquist plot usually displays two major features: (i) a standard semicircle at the high-frequency region that represents the bulk impedance; and, (ii) a vertical line representing the impedance of the interface between the electrolyte and electrode in the lower frequency region. The ionic conductivity κ of a solid electrolyte can be determined by

$$\kappa = \frac{1}{R_b} \cdot \frac{t}{S} \qquad (4.4)$$

where t is the thickness of the solid electrolyte thin film, S is the area of electrodes that contact the electrolyte film and R_b is the bulk resistance. R_b can easily be obtained directly from the Nyquist plot as a boundary between the high- and low- frequency end regions[49].

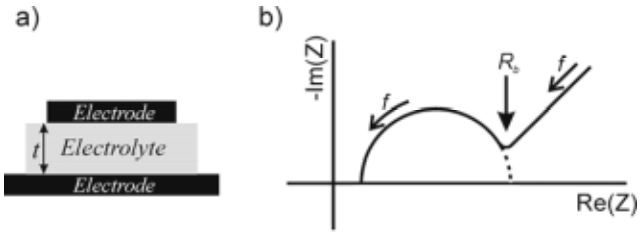

Figure 4.2. a) Two-probe setup. A current response is measured upon applying a voltage between to electrodes sandwiching an electrolyte of thickness *t*. b) An example of a typical Nyquist plot.

The conductivity of solid electrolytes can easily be measured using two- or four-probe techniques. In the four-probe technique, a current is driven between the two outer electrodes, while the voltage drop between the two inner electrodes is measured (figure 4.3). The ionic conductivity comes directly from

$$\kappa = j\,L / \Delta V \qquad (4.5)$$

where j is the current density (current divided by the thickness t and width w of the electrolyte), ΔV is the potential measured between the two inner electrodes, and L is the distance between them. The conductivity of the PSS:Na based electrolyte, measured using this four-probe configuration, is on the order of 10 μS cm^{-1} at 40% relative humidity[21].

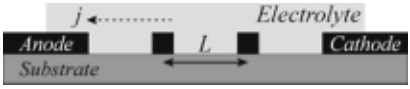

Figure 4.3. Four-probe setup. A voltage is applied between the anode and the cathode, and a potential difference is measured by the additional two probes separated by a distance *L*.

4.4 Electric double layer capacitors

An interesting feature of electrolytes is their ability to form electric double layer capacitors (EDLCs). As previously mentioned, electrolytes are electron insulators but ionic conductors. Upon contact with two oppositely charged ion-blocking electrodes sandwiching a common electrolyte (figure 4.4a), the anions migrate towards the anode, while the cations migrate towards the cathode (figure 4.4b). At the electrolyte/electrode interfaces, electrical double layers are then formed (figure 4.4c). The formed double layer can be seen as a two-plate capacitor separated by a distance of a few Ångstroms, typically the thickness of the first solvation shell around the ions. Because of this small distance, the capacitance of this model plate capacitor is large[43]. The resulting EDLCs' capacitance can reach high values, up to 500 μF cm^{-2}[59]. These capacitances are almost independent on the thickness of the electrolytes, since the capacitors are formed in the vicinity of the electrode surfaces. Thanks to charge separation that is formed within a few microseconds, EDLCs respond quickly to an applied electric field[43]. EDLCs can be characterized using impedance spectroscopy. The effective capacitance for a capacitor with poly(vinyl phosphonic acrylic acid) P(VPA-AA) electrolyte is of the order of 10 μF cm^{-2} at 100 Hz[60].

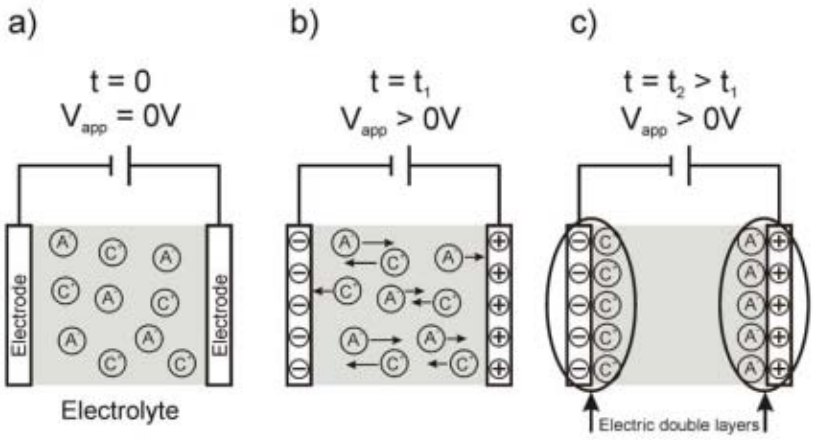

Figure 4.4. The principle of the electric double layer capacitor (EDLC). A common electrolyte is sandwiched between two ion-blocking electrodes. a) At time t = 0 with no potential difference between the electrodes, the ions are distributed uniformly in the electrolyte medium. b) Upon applying a voltage at $t = t_1$ anions (A^-) start to move towards the positively charged electrode, while the cations (C^+) move to the negatively charged electrode. c) After a while at $t_2 > t_1$, the ions start to pack near the electrode interfaces giving rise to formation of the electric double layer (EDL).

The structure of the electric double layer is commonly described by Gouy-Chapman-Stern (GCS) model[43]. The thicknesses of the double layer on the electrode and electrolyte sides are not the same, because the charges at both sides are confined differently. The interaction between solvated ions and the charged electrode is mostly electrostatic, while specific adsorption of ions may take place too. At the electrolyte side, the double layer consists of a compact (Helmholtz) layer of ions next to the electrode surface followed by a diffuse layer that extends into electrolyte bulk (figure 4.5). Ions at different positions in this diffuse layer do not have the same energy due to the variation of the electrostatic potential. Therefore the thickness of the diffuse layer will be varied when the potential profile across the layer is modified. As the electrode potential becomes higher, the diffuse layer becomes more compact. Also, the thickness is dependent on the ionic concentration of the electrolyte. Higher ionic concentration results in a less extended diffuse layer, i.e. the charges in the electrolyte become more tightly compressed

against the compact layer. According to this model, the double layer equivalent circuit is made of two capacitors in series with the capacitances representing the compact and diffuse layers. The potential profile (solid curve) through the electrode side of the double layer according to GCS model is shown in figure 4.5. The potential profile in the compact layer, shown in the figure 4.5, is linear because of the assumption of constant capacitance of this layer (according to Helmholtz model)[43].

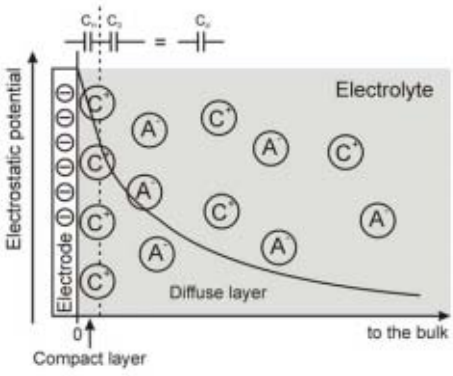

Figure 4.5. The arrangement of ions in the electric double layer (EDL) according to the Gouy-Shapman-Stern (GCS) model. The double layer is formed by a compact layer of ions next to the electrode followed by a diffuse layer extending into the bulk. The capacitance of the EDL (C_d) can be seen as the resulting capacitance from a series of two capacitors: the compact (C_H) and diffuse (C_D) layer capacitors. When $C_H >> C_D$, C_d is approximately equal to C_D. In constrast, at very high C_D, C_d is almost the same as C_H. The solid curve shows the variation of the electrostatic potential with distance from the electrode/electrolyte interface into the bulk.

5 Organic Field-Effect Transistors

Since their discovery in 1987[61], organic field-effect transistors (OFETs) have been intensively scrutinized and improved. Nowadays OFETs have started to find applications that other conventional inorganic transistors can not compete with. They serve as the main component in low-cost and flexible electronic circuits[62]. Their performance is now compared with that of amorphous silicon (a-Si:H) transistors, which are widely used in active matrix liquid crystal displays (LCDs). They offer a promising platform for many new opportunities e.g. for flexible display back planes[63,64] and integration of logic circuitry into low-cost electronic products[65]. Prototype radio frequency identification tags (RFID)[66-68] including OFETs are now coming close to entering the market.

5.1 Working principles

An OFET essentially consists of four different components: an electrical conducting material, an insulating material, an organic semiconducting material and a carrier substrate (figure 5.1a). The organic semiconducting film that connects two electrodes, the source and drain with a gap of length L and width W (channel dimension), is separated from a third electrode, the gate, by a thin film dielectric insulator. Upon charging the semiconducting channel, the structure formed by the semiconductor/insulator/gate resemble a two-plate capacitor. The conductivity of the semiconducting "plate" is altered by the voltage applied to the gate. Upon applying a voltage between the gate and the source (V_G), charges are injected from the grounded source electrode in the semiconductor and spread to charge the capacitor at the insulator/semiconductor interface resulting in a doped conductive channel. The density of the charges depends on the gate voltage.

The operation mode of the OFET is similar of conventional thin film FET[69], as illustrated in figures 5.1b-d. The channel conductance is mainly controlled by the potential on the gate. Since some of the induced charges are trapped in the electronic defect states in the semiconductor at the insulator/semiconductor interface, a certain voltage on the gate is required to account for the voltage drop that is caused by the traps. These traps should first be filled before the additional induced charges can be mobile and thus contributing to the current in the transistor. The voltage that is needed to compensate for any voltage drop at the insulator/semiconductor interface and to turn the transistor channel on is called the threshold voltage (V_T). Therefore the effective gate voltage becomes V_G - V_T. In some cases, an opposite voltage has to be applied to turn off the channel due to the bulk conductivity of the semiconductor layer at V_G = 0 V[70]. V_T originates also from the mismatch of the energy levels between the gate electrode, the insulator layer, and the semiconductor, due to the difference in work functions, which is referred to the flat-band voltage. When a small V_D is applied, the drain current (I_D) follows Ohm's law, i.e. the channel conductance is constant. This is the linear regime (figure 5.1b). As V_D increases and reaches a value close to V_G, the electric potential at the dielectric-semiconductor interface is almost constant in the channel region close to the drain. This results in a reduction of the thickness of the channel next to the drain. When V_D reaches a value equal to the effective gate voltage, the channel is pinched off, i.e. the channel thickness is reduced to zero. The current saturates (figure 5.1c) and is limited by this reduced channel region where the electric field along the channel is the highest. Further increase of V_D does not give rise to current increase, but it broadens the reduced region. Because the potential at the pinch-off point remains constant and equals to $V_D = V_G - V_T$, the potential drop between the source and the point approximately is the same. This will result in saturation of the drain current ($I_{D,sat}$) (figure 5.1d).

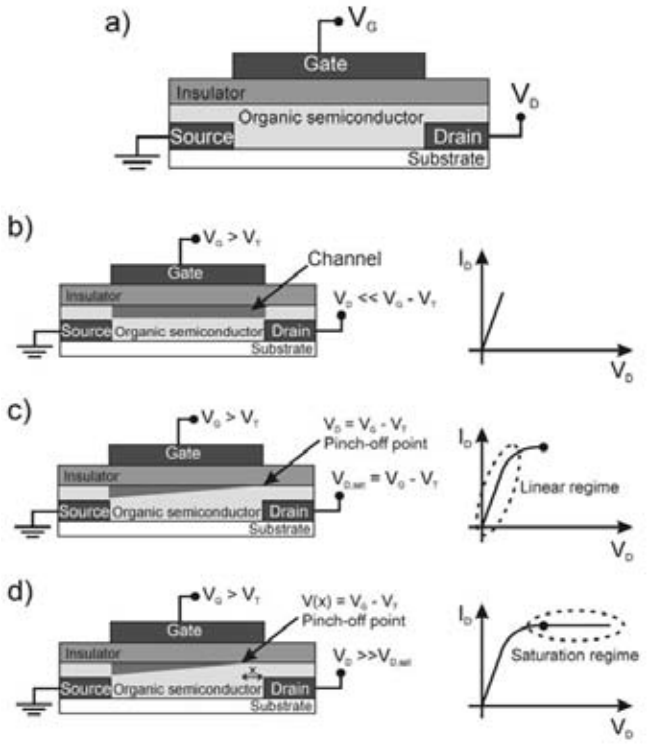

Figure 5.1. Illustrations of the operating regimes of an organic field-effect transistor (OFET) with corresponding current-voltage output characteristics. a) With no applied voltages (V_D and V_G) at drain and gate electrodes. b) The linear regime. c) The channel is pinched off and starts of the saturation regime. d) The saturation regime. The level of the saturation current is altered by varying the gate voltage.

5.2 Device structures and semiconductor materials

The OFET can be made in different device structures depending on the physical nature of both the semiconductor and the insulator. Even if the same components are used, the behavior of the device also depends on the transistor geometry[71]. The most commonly found OFET's structures (in addition to the structure shown in figure 5.1) are illustrated in figure 5.2. The differences of these structures lie on the position of the channel with respect to the source-drain contacts. For instance, the charges are directly injected into the channel at semiconductor/dielectric interface in a bottom

contact/bottom gate configuration (figure 5.2a) while they first have to travel through the undoped semiconductor before they reach the channel in the top contact/bottom gate (figure 5.2c). For all structures, plastic substrates such as polyethylene and polyester can be used to make the transistor mechanically flexible. Electrodes can also be made from organic-based conductors such as PEDOT:PSS and polyaniline after solution processing.

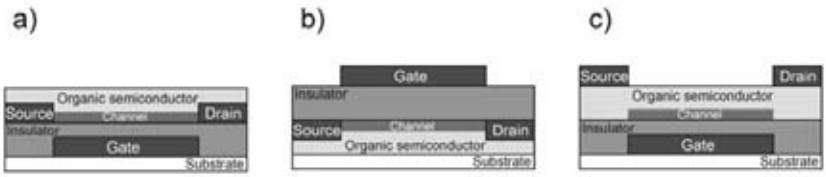

Figure 5.2. Common device structures of OFETs. a) Bottom contact, bottom gate. b) Top contact, top gate. c) Top contact, bottom gate. The position of the 1-2 nm-thick channel is at the semiconductor/insulator interface within the gray rectangular area.

There are two classes of materials that are used as organic semiconductors, conjugated small molecules and polymers[72]. Polymers due to their high molecular weight cannot be sublimed in vacuum and condensed on a substrate. Hence, polymers are processed from solution. Some polymer films can posses up to 70% of crystalline domains. Small molecules like pentacene can be vacuum sublimed. An optimized choice of substrate temperature can lead to a single crystal. Depending on the polarization of the gate, either electrons or holes accumulate in the channel, which is called respectively n-channel or p-channel. The electron donor or acceptor characters of the semiconductors make then easier to form, respectively, a p- or n-channel. Figure 5.3 shows examples of some molecular and polymeric p- and n-channel semiconductors. Most of the reported organic transistors are p-channel transistors[72], because of its high stability under ambient conditions and under bias stress. One major problem with n-channel transistors has been the overwhelming trapping effect at the dielectric-insulator interface, as well as their unstability in presence of water and dioxygen. Thus, n-channel transistors only can operate when processed and tested under inert

conditions. A second challenge with n-channel transistors is the electron injection into the LUMO level of the organic semiconductor from an electrode[73]. The work function of the metal electrode should be low enough to promote easy electron injection in the LUMO level of the organic semiconductor. For instance, gold electrode is suitable for hole injections, while it is less appropriate to n-channel transport because of its high work function, giving rise to high injection barrier for electrons at the contacts. Therefore low work function metals, such calcium, are preferred for n-channel transistors. Unfortunately, these kinds of metals become easily oxidized in air. In some cases, OFET exhibits both n- and p-channel behavior depending on the polarity of both V_D and V_G and the transistor is called ambipolar[73].

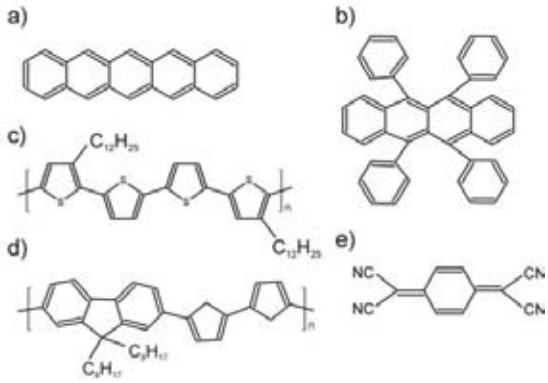

Figure 5.3. Chemical structures of some organic semiconductors. a) Pentacene. b) Rubrene. c) PQT-12 (poly(3,3'''-didodecylquaterthiophene)). d) F8T2 (poly(9,9dioctyl-fluorene-alt-bithiophene)). e) TCNQ. Pentacene and rubrene are small conjugated molecules, while PQT-12 and F8T2 are conjugated polymers. These are p-type materials. However, TCNQ is an n-type semiconducting material.

5.3 OFET characteristics

The conductivity of the channel increases upon applying a gate bias because OFETs normally operate in the accumulation mode. The general trends in OFET characteristics are usually illustrated via conventional semiconductor

theory[69]. The relationships between the current and voltage for the transistor's different operating regimes have analytically been derived by assuming the gradual channel approximation: the electric field at the semiconductor/insulator interface is much higher than that along the channel, between source and drain, which is fulfilled when the channel length is larger than the insulator thickness. These are given by:

$$I_{D,linear} = (W/L)\mu_{linear} C_i \left(V_G - V_T - (V_D/2)\right)V_D \qquad (5.1a)$$

$$I_{D,saturation} = (W/2L)\mu_{saturation} C_i \left(V_G - V_T\right)^2 \qquad (5.1b)$$

where $I_{D,linear}$ and $I_{D,saturation}$ are the drain currents in, respectively, the linear and saturation regimes. W and L are the channel width and length, C_i is the capacitance per unit area of the insulator layer, μ_{linear} and $\mu_{saturation}$ are the linear and saturation field-effect mobility. Figure 5.4a shows typical output characteristics, i.e. I_D versus V_D for different V_G, of a p-type channel OFET. From output characteristics the linear and saturation regimes become clearly visible.

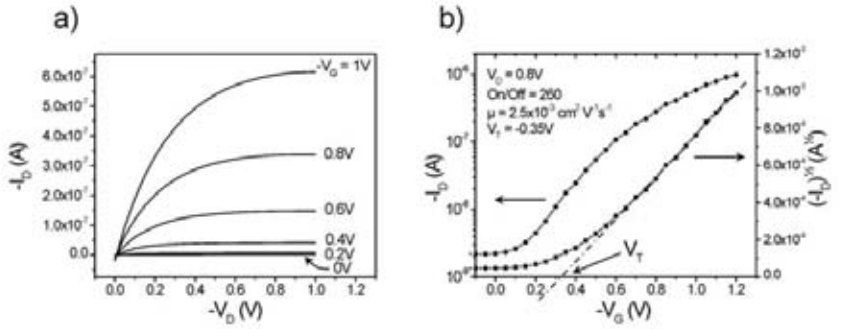

Figure 5.4. Typical current-voltage characteristics of a p-type OFET. The channel length and width was 3.5 μm and 200 μm. a) Output characteristics. b) Transfer characteristics in the saturation regime, indicating the threshold voltage V_T determined from the linear fit to the square root of the drain current that intersects the x-axis.

The charge carrier mobility is one of the most important parameters for a material used in an OFET. It quantifies the average drift velocity of a charge carrier per unit electric field. High mobility is desirable because it gives higher output currents and improves the response time of the transistors upon gate bias stress. The mobility can be affected by many factors. It varies with the nature of the semiconductor and the fabrication methods. For instance, the mobilities of pentacene and P3HT thin films are not the same even for similar device configuration. Pentacene, which is vacuum deposited, has higher mobility (1.5 $cm^2\ V^{-1}s^{-1}$)[74,75] than regio-regular P3HT (0.1 $cm^2\ V^{-1}s^{-1}$)[34], which is directly processed from a solution. The purity and the degree of crystallinity of the material (influenced by the solvent and the deposition method) affect significantly the mobility. Annealing the film after deposition by spin-coating has been shown to give rise systematically to higher mobility due to (i) the complete removal of solvent in the semiconductor films, (ii) the increased molecular packaging[76,77]. From the equation 5.1a and b, the linear and saturation mobilities can directly be calculated by differentiating I_D with respect to V_G:

$$\mu_{linear} = \left(\frac{\partial I_{D,linear}}{\partial V_G} \right) \left(\frac{L}{W C_i V_D} \right) \qquad (5.2a)$$

$$\mu_{saturation} = \left(\frac{\partial (I_{D,saturation})^{½}}{\partial V_G} \right) \left(\frac{2L}{W C_i} \right)^{½} \qquad (5.2b)$$

Figure 5.4b shows a semilog plot of I_D and square root of I_D versus V_G at constant V_D in the saturation regime called transfer characteristics. The saturation mobility can easily be calculated by extracting the gradient of the square root of I_D. From transfer characteristics threshold voltage (V_T) can be obtained by a linear fit to the square root of I_D that intersects with the V_G-axis. In the linear regime, V_T can be determined from a double derivation of I_D at low V_D with respect to V_G[78]. Other important parameters that can be

extracted from the transfer characteristic is the on/off current ratio, the ratio between I_D in the on-state (at particular V_G) and I_D in the off-state (at V_G = 0V), $I_{D,on}/I_{D,off}$. High on/off current ratio is required for the transistor to be integrated in circuits. The on/off ratio for P3HT based transistor was obtained as high as 10^6[79].

5.3.1 Gate voltage dependent mobility

In a transistor the mobility varies with gate voltage[80]. To detect the voltage dependence, the mobility should be measured in the linear regime where the charge distribution is uniform in contrast to the saturation regime, where the potential along the channel varies. Gate voltage dependence is related to the fact that the mobility is carrier density dependent. The increase of the gate voltage results in an increase of the carrier concentration, which in turn gives rise to an increase of mobility. Some models have been reported to account for gate voltage dependent mobility. For instance, in the multiple trapping and release model[81], it is assumed that there exist trap states nearby the transport band edge. When a gate voltage is applied, the potential drop at the insulator/semiconductor interface leads to a reduction of the energy distance between the trap states and the transport band edge, resulting in an easy release of the trapped carriers, which in turn increases the mobility. This model is applied to well-ordered systems. For disordered systems the gate bias dependency is described by a variable-range hopping model[82] and the occupation of the Gaussian density of state; where the Gaussian width accounts for the energy disorder level. Upon applying a gate voltage, the accumulated charge carriers in the semiconductor layer close to the insulator will fill the lower lying states of the Gaussian distribution. An increase of charge carrier density leads to a reduction of the energy hop that the charge carriers need to realize to access the transport energy level (close to the max of the Gaussian). Any additional charges will instead occupy relatively high energy states and require less activation energy to hop to a neighboring site resulting in higher mobility with increasing the gate voltage.

Note that if the mobility is gate voltage dependent, the equations 5.1a and b can be used but it is needed to report the V_G when discussing the mobility.

5.3.2 Contact resistance

Contact resistances between the organic semiconductor and the metal electrodes play an important role in electronic charge injection in OFETs. These effects are more dominant in short channel length devices and therefore have to be taken into account when extracting the mobility from the characteristics of the device. Omitting these corrections will give an underestimate of the true channel mobility. The key feature of contact resistance (R_C) is the non-linear increase of I_D at low V_D. It originates from the energy barrier formed at the interface between the metal and the semiconductor, and from lower mobility region of the semiconductor film adjacent to the electrodes (compared to the rest of the polymer layer)[83]. Therefore, the reduction of R_C can be made by matching the work function of the electrodes with the ionization potential of the polymer. It should be noted that the role of contacts in bottom and top contact (BC and TC) transistors affect R_C. R_C is more pronounced in BC transistor compared to TC transistor, the deposition of metal on top of the semiconductor usually leads to a more intimate contact because of a partial diffusion of metal atoms into the semiconductor[84,85]. Because of the voltage drop at the contacts, the current-voltage characteristics deviate from conventional equations previously mentioned. To account for R_C at the electrodes, the voltage drop through the contact resistance (I_DR_C) is added in equation 5.1a as the difference between V_D and I_DR_C[80], and is given by the total width-normalized resistance

$$R\,W = \frac{L}{C_i \mu (V_G - V_T)} + R_C\,W \qquad (5.3)$$

R_C can be extracted using the transfer line method[86]. The resistance is measured in the linear regime for similar devices with various channel

lengths. The measured resistance is a sum of both channel and contact resistances and proportional to L. R_C is defined by the intercept of the line at $L = 0$. In addition, the slope of the curve in a RW vs. L plot gives the mobility, which usually is found out to be gate voltage dependent[86].

5.3.3 Time response

In addition to the current-voltage characteristics, the time response of a transistor is of tremendous importance for applications in electronics. For vanishingly small stray capacitance (overlap between source or drain and gate), the speed of a transistor is limited by the transit time (t_{tr}) of the charge carriers from the source electrode through the channel to the drain electrode[69], and is given by $L^2/\mu V_D$. This provides the maximum switching frequency ($f_{max} = 1/t_{tr}$) called cut-off frequency, of a single transistor. For organic integrated circuits, the switching speed is governed by the performance of the individual transistors. To reach higher speeds, higher mobility materials are therefore important, as well as scaling down the transistor geometries. However other device parameters also affect considerably the effective field effect mobility: (i) contact resistance, (ii) grains boundaries in the organic layers, (ii) charge trapping at the semiconductor/dielectric interface, (iv) dielectric constant of the insulating layer; (v) the roughness of the semiconductor/dielectric interface. In order to create a fast circuit, other parameters come into play: thicknesses of the various layers in the circuit, stray capacitance between gate and source/drain, and circuit design. For all those reasons, organic transistors and circuits appear to be able to run at very different frequencies: solution processed ring oscillators have an oscillation frequency in order of 1-10 Hz[87], while conventional processed polymer oscillators show switching frequencies of a kHz region[88].

5.4 Electrolyte-gated OFETs

In early studies, transistors were fabricated mostly to characterize materials. Most of organic semiconductor properties in OFET have been characterized using thermally grown SiO_2 as the insulator because of its ready availability. With the improvement of organic semiconductors, OFETs became a potential technology. Hence, researchers have started to optimize the device itself. An important challenge is to reduce the operation voltage while keeping as high output current as possible. In order to achieve that, the capacitance (per area) of the insulator C_i (equation 5.1) should be high. The capacitance depends on both the dielectric constant (k) and the thickness of the insulator. Various kinds of insulators with high capacitance have been investigated[89]: inorganic insulating materials with high k such as aluminum oxide (Al_2O_3, k = ~10) and titanium oxide (TiO_2, k = ~41), and polymeric dielectric materials such as polyvinylalcohol (PVA, k = ~10) and polyvinylphenol (PVP, k = ~4). The other approach is to reduce the insulator thickness. Self-assembled monolayers (SAM) with a thickness of one molecular monolayer (~2 nm) have been used as a gate dielectric to reach a capacitance of about 1 μF cm^{-2}[90].

The insulating materials should also fulfill demands specific to organic electronics, i.e. low-cost, compatible with flexible substrates, processible from solutions, insoluble in the solvent used for deposition of the organic semiconductor, and compatibility with the gate electrode materials. Electrolytes have been found to be great materials to gate transistors (figure 5.5a)[60,91-97]. These types of dielectrics are usually composed of a salt distributed in a solution or matrix, e.g., polymer gel. When a gate potential is applied, the ions in the electrolyte redistribute and migrate into the semiconductor leading to electrochemical doping (dedoping) in the bulk of the organic semiconductor. Thus, the channel is opened (closed). These transistors are classified as electrochemical (EC) transistors (figure 5.5b). They can typically operate at low drive voltages (< 2 V) and be processed using low-cost production techniques. However, they respond slowly. One of

the successful EC transistors has been reported by Nilsson et al[94]. Their transistor is based on lateral architecture where the electrodes consisted only of a thin film of PEDOT:PSS, while a calcium chloride based gel is the electrolyte. The area covered with the electrolyte between the source and drain defined the channel. This resulted in an all-organic EC transistor. For this device, the conductivity of the channel decreased upon applying a gate voltage because of the reduction of the PEDOT:PSS channel, thus the on-state is defined at zero applied gate voltage.

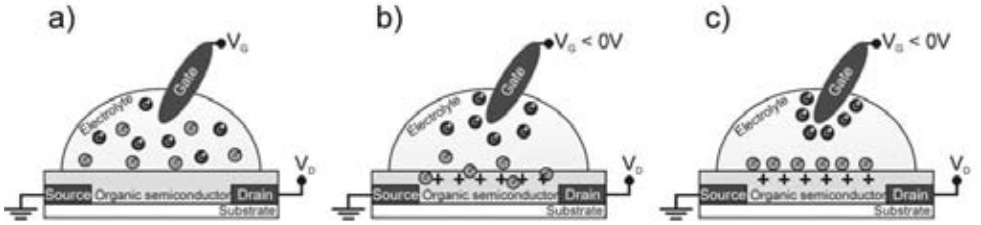

Figure 5.5. An illustration of an organic transistor gated via an electrolyte. a) When no voltage is applied to the gate, the ions in the electrolyte are distributed uniformly. b) Upon applying a negative gate bias, ions respond to the electric field and redistribute. The migration of anions into the semiconductor causes electrochemical doping and opens the channel. This is the typical behavior of an electrochemical transistor. c) If electrochemistry is prevented because the anions are prevented to migrate into the semiconductor film, electrostatic charge injection instead will take place in response to the high electric filed across the electric double layer formed at electrolyte/semiconductor interface. The transistor works as a field-effect transistor.

Solid polymer electrolytes have also been used in gating organic transistors[92,98]. For example poly(ethylene oxide) (PEO) with dispersed lithium perchlorate salt has been demonstrated as gate insulator material. The motion of the anions into the semiconductor is remarkably reduced when the transistor operates in vacuum, thus preventing bulk electrochemistry to occur. Electrostatic charge injection takes place at the source-semiconductor interface in response to the high electric field created at the interface between polymer semiconductor and polymer electrolyte

(figure 5.5c)[98]. Upon operation in air, current modulation resembles EC transistors. Because of bulk electrochemistry the conductivity of the channel of these transistors in off-state after device operation is higher compared to off-state before turning the transistor on[60]. The use of polymer electrolytes has allowed injection of high carrier density (10^{14} – 10^{15} charges cm^{-2}) and the achievement of metallic conductivities in the channel of polymer electrolyte-gated OFET[92]. It also enables n-channel operation[95].

In order to avoid the electrochemical doping of the bulk semiconducting polymer film when operating at ambient atmosphere, solid state polyanionic proton conducting electrolytes such as the random copolymer of vinyl phosphonic acid and acrylic acid, P(VPA-AA) can be used as gate material[60,96]. By applying a negative electric potential to the gate, protons migrate towards the gate electrode and form an electric double layer at polyelectrolyte/electrode interface. The remaining immobile polyanion chains stay close to the positively doped organic semiconductor, allowing the formation of p-channel. Because the polyanionic chains are immobile, they cannot penetrate the semiconductor layer, thus preventing electrochemistry in the bulk of the channel. Unlike EC transistors that require several of seconds to switch, OFETs gated via electric double layer capacitor (EDLC-OFET) exhibit transients in kilohertz region. The quick formation of double layers at polyelectrolyte/electrode and polyelectrolyte/semiconductor interfaces result in low voltage operation (< 1 V) and high output current (in μA range for L/W = 7/200). Employing polyelectrolytes as gate insulator, the thickness of the insulator and the position of gate electrode become less important since the EDLC spontaneously forms at insulator/semiconductor interface upon applying a gate bias[60]. As a result, the devices could be produced cheaply via e.g. printing techniques.

5.5 Applications of OFETs

Organic transistors are essential building blocks in most electronic and optoelectronic applications. The transistor is required to control the current flow to and from a specific device. In an active addressed display, transistors are implemented as switches to activate individual pixels. Integrated smart pixel with an OFET switching an organic light-emitting diode (OLED) pixel has been demonstrated[99,100]. The OFET performs signal processing, while the OLED converts the electrical signal into optical output. The integration of both components on the same substrate would contribute to a simpler and cheaper manufacturing process to produce all-organic active OLED displays on flexible polymeric substrates[63,101]. In addition, analog and digital circuits that use OFET, such as inverters and ring oscillators, have also been reported[65,102,103].

There are two transistor operation modes depending on how the channel conductance is modulated. When the channel conductance at zero gate bias is very low, an applied gate voltage is required to form the channel. This type is the normally-off channel transistor, i.e. enhancement (accumulation) mode operation. However, if a gate bias is needed to reduce the channel conductance because it already exits at zero gate bias, the transistor is known as normally-on, i.e. depletion mode operation. For various kinds of display applications, the enhancement mode device is very attractive because of its low power consumption. For instance, an all-organic active matrix addressed display based on smart pixel and made on flexible substrates has been reported by Andersson et al[19,104]. Each individual smart pixel device includes a depletion mode transistor. The transistors are updated row by row, while the display cells are updated column wise. When updating only the first row, transistors in this row are kept conducting and the remaining transistors in other rows are switched to their off-state by applying the gate voltage. After an update the transistors are switched back to their closed state and the information is stored in the matrix display. This kind of updating process, however, will lead to stress and degrade the

transistors, and will require high power consumption as well. The use of enhancement mode transistors in the active matrix displays would prevent those issues.

The type of the pixel used in the active matrix displays will determine the maximum cut-off frequency of the transistor that is required when updating the pixel itself. For example, displays using electronic ink (contains black and white sub-micron particles with opposite charge in a transparent fluid) switch at speeds in order of 200-250 ms (4-5 Hz), which is sufficient for electronic paper[105,106]. However, for video-rate switching, the display has to be refreshed at 60 Hz, which means that the active transistor should have a response time very much shorter than 16.7 ms, i.e. in order of 100 μs[107]. One type of pixel that fulfills the requirement to display moving picture is based on the OLED. OLEDs are current driven devices, and the brightness uniformity depends on the uniformity of drive transistor characteristics. In active matrix OLED display, each individual pixel is controlled by one or more transistor. A common design of such pixel contains two transistors, a select transistor and a drive transistor[101]. The most significant requirement for the transistor is to supply sufficient current to achieve appropriate brightness. The select transistor's task is to charge the storage capacitor that holds the gate voltage constant for the drive transistor during the complete frame time. In addition, it should be noted that the gate capacitor of the transistor plays an important role in circuits. If the transistor has a large capacitance, then it is needed to send a lot of charge to the gate to switch on the transistor in a circuit. The time that takes for charging the gate will introduce a gate delay, which results in lowering the circuits speed. However, if the charge comes from another transistor that has high current throughput, then the time delay will be reduced.

6 Conclusions

This thesis deals with organic semiconductor–based devices whose working mechanism involves electrolytes. When a semiconductor in an electronic device is polarized in contact with an electrolyte, ions reorganize at the semiconductor-electrolyte interface. Ions accumulate in the electrolyte at the interface with the semiconductor, and charge carriers (electrons or holes) of the opposite charge belonging to the semiconductor migrate towards the interface with the electrolyte. This interface polarization creates electric double layers, also called Helmholtz double layers. At that stage, the ions can or cannot penetrate into the semiconductor depending on the chemical nature of the ions and the chemical nature of the semiconductor. In this thesis, we have varied the ions and the semiconductors to investigate experimentally the fate of the electric double layers. We have mostly focused on using the right combination of materials (electrolyte-semiconductor) to create new devices that can be used either to analyze phenomenon or find applications in electronics.

The first electrolyte-semiconductor system studied was made of small mobile ions that can penetrate into an organic semiconductor made of a conducting polymer. In a polymer semiconductor, the interchain interactions are weak (mostly Van der Waals) such that ions can easily penetrate into it. In that case, electrochemistry takes place moving the double layer into the organic semiconductor. Upon this electrochemical doping, the organic semiconductor changes color. This electrochromic response was used to study the transport of charge in electrolytes. The direction and the magnitude of the electric field along an electrolyte can be quantified by

measuring electrochromism induced by the field in isolated segments of conjugated polymer films in contact with the electrolyte.

A different kind of behavior is found in the case of inorganic semiconductors. Indeed, the bonds between the atoms in such a material are strong (covalent bonds), such that the penetration of ions into a polarized inorganic semiconductor is negligible. A theoretical study of the electrostatic potential within a so-called *pen*-heterojunction made up of two semi-infinite, doped semiconductor media separated by an electrolyte region is reported.

One of the main fundamental questions in this work has been the following: "Is it possible to have a polarized electrolyte-organic semiconductor interface without penetration of ions in the organic semiconductor (i.e. without bulk electrochemical doping)?" Since, all organic semiconductors are molecular (or polymeric) solids made of molecules (or polymer chains) weakly interacting, it is impossible to increase the molecular interaction to the degree that ion penetration is completely hindered. Hence, another strategy was proposed: use of large immobile polymeric ions that wouldn't be expected to penetrate into the weakly bound organic semiconductors. With that approach, a new generation of organic field-effect transistors gated via an electric double layer capacitor has been demonstrated when an acidic polyanionic proton conductor is used. The large capacitance of the double layer formed at electrolyte/organic semiconductor interface enables the low operation voltage and the fast response of the transistor. The effect of the ionic currents on the performance of a polyelectrolyte-gated organic field-effect transistor is investigated by varying the relative humidity of the device ambience. Below 40% humidity, hydrolysis is negligible and the transistors performances are optimum. The transistor operates below 1 V and its conducting channel is formed in approximately 50 μs.

In the last part, we continue to move towards applications and realized a monolithic integration of the electrolyte-gated organic field-effect transistor and an organic electrochromic pixel in a smart pixel for a novel type of display. The main advantages compared to the state of the art electrochemical smart pixel (using an electrochemical transistor) are a shorter switching time, the enhancement mode operation, in combination with low voltage operation in both the transistor and the pixel, which enables the low power consumption important for display applications.

7 References

[1] www.plasticlogic.com, (2008).

[2] J. H. Burroughes, D. D. C. Bradley, A. R. Brown, R. N. Marks, K. Mackay, R. H. Friend, P. L. Burns, and A. B. Holmes, Nature **347,** 539-541 (1990).

[3] Q. Pei, G. Yu, C. Zhang, Y. Yang, and A. J. Heeger, Science **269,** 1086-1088 (1995).

[4] R. J. Young and P. A. Lovell, *Introduction to Polymers*, Second ed. (Chapman & Hall, 1991).

[5] J. W. D. Callister, *Materials Science and Engineering, An Introduction*, Seventh ed. (Wiley, 2007).

[6] P. Atkins and L. d. Paula, *Physical Chemistry*, Vol. Seventh (Oxford, 2002).

[7] W. R. Salaneck, R. H. Friend, and J. L. Bredas, Physics Reports **319,** 231-251 (1999).

[8] A. J. Heeger, Angewandte Chemie International Edition **40,** 2591-2611 (2001).

[9] C. K. Chiang, C. R. Fincher, Y. W. Park, A. J. Heeger, H. Shirakawa, E. J. Louis, S. C. Gau, and A. G. MacDiarmid, Physical Review Letters **39,** 1098 (1977).

[10] W. P. Su, J. R. Schrieffer, and A. J. Heeger, Physical Review Letters **42,** 1698 (1979).

[11] A. O. Patil, A. J. Heeger, and F. Wudl, Chem. Rev. **88,** 183-200 (1988).

[12] M. Jaiswal and R. Menon, Polymer International **55,** 1371-1384 (2006).

[13] A. Moliton and R. C. Hiorns, Polymer International **53,** 1397-1412 (2004).

[14] A. J. Epstein, *Insulator-Metal Transition and Metallic State in Conducting Polymers*, Vol. I (CRC Press, New York, 2007).

[15] A. A. Argun, P. H. Aubert, B. C. Thompson, I. Schwendeman, C. L. Gaupp, J. Hwang, N. J. Pinto, D. B. Tanner, A. G. MacDiarmid, and J. R. Reynolds, Chem. Mater. **16,** 4401-4412 (2004).

[16] R. J. Mortimer, A. L. Dyer, and J. R. Reynolds, Displays **27,** 2-18 (2006).

[17] P. R. Somani and S. Radhakrishnan, Materials Chemistry and Physics **77,** 117-133 (2003).

[18] C. Carlberg, X. Chen, and O. Inganäs, Solid State Ionics **85,** 73-8 (1996).

[19] P. Andersson, D. Nilsson, P. O. Svensson, M. Chen, A. Malmström, T. Remonen, T. Kugler, and M. Berggren, Advanced Materials **14,** 1460-1464 (2002).

[20] H. W. Heuer, R. Wehrmann, and S. Kirchmeyer, Advanced Functional Materials **12,** 89-94 (2002).

[21] E. Said, N. D. Robinson, D. Nilsson, P. O. Svensson, and M. Berggren, Electrochemical and Solid-State Letters **8,** H12-H16 (2005).

[22] L. B. Groenendaal, F. Jonas, D. Freitag, H. Pielartzik, and J. R. Reynolds, Advanced Materials **12,** 481-94 (2000).

[23] Orgacon™EL350, (http://www.agfa.com/docs/sp/sfc/OrgaconEL350_datasheet.pdf).

[24] J. C. Gustafsson-Carlberg, O. Inganas, M. R. Andersson, C. Booth, A. Azens, and C. G. Granqvist, Electrochimica Acta **40,** 2233-2235 (1995).

[25] T. Johansson, L. A. A. Pettersson, and O. Inganäs, Synthetic Metals **129,** 269-274 (2002).

[26] X. Crispin, F. L. E. Jakobsson, A. Crispin, P. C. M. Grim, P. Andersson, A. Volodin, C. vanHaesendonck, M. VanderAuweraer, W. R. Salaneck, and M. Berggren, Chem. Mater. **18,** 4354-4360 (2006).

[27] N. D. Robinson, P.-O. Svensson, D. Nilsson, and M. Berggren, Journal of The Electrochemical Society **153,** H39-H44 (2006).

[28] J. Z. Wang, Z. H. Zheng, H. W. Li, W. T. S. Huck, and H. Sirringhaus, Nat Mater **3,** 171-176 (2004).

[29] F. L. E. Jakobsson, X. Crispin, L. Lindell, A. Kanciurzewska, M. Fahlman, W. R. Salaneck, and M. Berggren, Chemical Physics Letters **433,** 110-114 (2006).

[30] E. Frackowiak, V. Khomenko, K. Jurewicz, K. Lota, and F. Beguin, Journal of Power Sources **153,** 413-418 (2006).

[31] L.-J. Her, J.-L. Hong, and C.-C. Chang, Journal of Power Sources **157,** 457-463 (2006).

[32] Z. Bao, A. Dodabalapur, and A. J. Lovinger, Applied Physics Letters **69,** 4108-4110 (1996).

[33] M. Jeffries-El and R. D. McCullough, *Regioregular Polythiophenes*, Vol. 1 (CRC Press, New York, 2007).

[34] H. Sirringhaus, P. J. Brown, R. H. Friend, M. M. Nielsen, K. Bechgaard, B. M. W. Langeveld-Voss, A. J. H. Spiering, R. A. J. Janssen, E. W. Meijer, P. Herwig, and D. M. de Leeuw, Nature **401,** 685-688 (1999).

[35] R. J. Kline, M. D. McGehee, E. N. Kadnikova, J. Liu, and J. M. J. Fréchet, Advanced Materials **15,** 1519-1522 (2003).

[36] A. G. MacDiarmid, Angewandte Chemie International Edition **40,** 2581-2590 (2001).

[37] H. Shirakawa, A. McDiarmid, and A. Heeger, Chemical Communications**,** 1-4 (2003).

[38] K. Lee, S. Cho, S. Heum Park, A. J. Heeger, C.-W. Lee, and S.-H. Lee, Nature **441,** 65-68 (2006).

[39] B. H. Kim, D. H. Park, J. Joo, S. G. Yu, and S. H. Lee, Synthetic Metals **150,** 279-284 (2005).

[40] T. G. Backlund, H. G. O. Sandberg, R. Osterbacka, H. Stubb, T. Makela, and S. Jussila, Synthetic Metals **148,** 87-91 (2005).

[41] T. Lindfors and A. Ivaska, Journal of Electroanalytical Chemistry **531,** 43-52 (2002).

[42] C. Y. Wang, V. Mottaghitalab, C. O. Too, G. M. Spinks, and G. G. Wallace, Journal of Power Sources **163,** 1105-1109 (2007).

[43] E. Bard and L. Faulkner, *Electrochemical Methods: Fundamentals and Applications* (Wiley, New York, 2001).

[44] J. Y. Song, Y. Y. Wang, and C. C. Wan, Journal of Power Sources **77,** 183-197 (1999).

[45] B. E. Conway, *Electrochemical Supercapacitors: Scientific Fundamentals and Technological Applications* (Kluwer Academic / Plenum Publishers, New York, 1999).

[46] C. Xu, L. Liu, S. Legenski, M. Le Guilly, M. Taya, and A. Weidner, in *Enhanced smart window based on electrochromic (EC) polymers*, San Diego, CA, United States, 2003 (The International Society for Optical Engineering), p. 404-411.

[47] M. M. Mench, C. Y. Wang, and M. Ishikawa, Journal of the Electrochemical Society **150,** A1052-A1059 (2003).

[48] F. M. Gray, *Solid Polymer Electrolyte—Fundamentals and Technological Applications* (VCH Publishers, New York, 1991).

[49] X. Qian, N. Gu, Z. Cheng, X. Yang, E. Wang, and S. Dong, Journal of Solid State Electrochemistry **6,** 8-15 (2001).

[50] K.-H. Lee, J.-K. Park, and H.-D. Kim, Journal of Polymer Science Part B: Polymer Physics **34,** 1427-1433 (1996).

[51] J. T. Singh and S. V. Bhat, Bulletin of Materials Science **26,** 707-714 (2003).

[52] F. B. Dias, L. Plomp, and J. B. J. Veldhuis, Journal of Power Sources **88,** 169-191 (2000).

[53] M. Saboormaleki, A. R. Barnes, and W. S. Schlindwein, in *Characterization of Polyethylene Oxide (PEO) based polymer electrolytes*, San Antonio, TX, 2004, p. 726.

[54] A. M. Stephan, European Polymer Journal **42,** 21-42 (2006).

[55] J. L. Barrat and F. Joanny, in *Advances in Chemical Physics*, edited by S. A. R. I. Prigogine (2007), p. 1-66.

[56] F. Bordi, C. Cametti, and R. H. Colby, Journal of Physics Condensed Matter **16,** 1423-1463 (2004).

[57] D. Nilsson, T. Kugler, P.-O. Svensson, and M. Berggren, Sensors and Actuators B: Chemical **86,** 193-197 (2002).

[58] R. A. Robinson and R. H. Stokes, *Electrolyte Solutions*, Second ed. (Dover publications, INC, Mineola, New York, 2002).

[59] S. Mitra, A. K. Shukla, and S. Sampath, Journal of Power Sources **101,** 213-218 (2001).

[60] L. Herlogsson, X. Crispin, N. D. Robinson, M. Sandberg, O. J. Hagel, G. Gustafsson, and M. Berggren, Advanced Materials **19,** 97-101 (2007).

[61] H. Koezuka, A. Tsumura, and T. Ando, Synthetic Metals **18,** 699-704 (1987).

[62] Y. Sun, Y. Liu, and D. Zhu, Journal of Materials Chemistry **15,** 53-65 (2005).

[63] G. H. Gelinck, H. E. A. Huitema, E. van Veenendaal, E. Cantatore, L. Schrijnemakers, J. B. P. H. van der Putten, T. C. T. Geuns, M. Beenhakkers, J. B. Giesbers, B.-H. Huisman, E. J. Meijer, E. M. Benito, F. J. Touwslager, A. W. Marsman, B. J. E. van Rens, and D. M. de Leeuw, Nat Mater **3,** 106-110 (2004).

[64] H. E. A. Huitema, G. H. Gelinck, J. B. P. H. van der Putten, K. E. Kuijk, C. M. Hart, E. Cantatore, P. T. Herwig, A. J. J. M. van Breemen, and D. M. de Leeuw, Nature **414,** 599-599 (2001).

[65] H. Klauk, U. Zschieschang, J. Pflaum, and M. Halik, Nature **445,** 745-748 (2007).

[66] P. F. Baude, D. A. Ender, T. W. Kelley, M. A. Haase, D. V. Muyres, and S. D. Theiss, in *Organic semiconductor RFID transponders*, 2003, p. 8.1.1-8.1.4.

[67] R. Rotzoll, S. Mohapatra, V. Olariu, R. Wenz, M. Grigas, K. Dimmler, O. Shchekin, and A. Dodabalapur, Applied Physics Letters **88,** 123502 (2006).

[68] V. Subramanian, J. M. J. Frechet, P. C. Chang, D. C. Huang, J. B. Lee, S. E. Molesa, A. R. Murphy, D. R. Redinger, and S. K. Volkman, Proceedings of the IEEE **93,** 1330-1338 (2005).

[69] S. M. Sze, John Wiley Sons (1981).

[70] S. Kobayashi, T. Nishikawa, T. Takenobu, S. Mori, T. Shimoda, T. Mitani, H. Shimotani, N. Yoshimoto, S. Ogawa, and Y. Iwasa, Nature Materials **3,** 317-322 (2004).

[71] H. Sirringhaus, Advanced Materials **17,** 2411-2425 (2005).

[72] A. Facchetti, Materials Today **10,** 28-37 (2007).

[73] J. Zaumseil and H. Sirringhaus, Chem. Rev. **107,** 1296-1323 (2007).

[74] H. Klauk, M. Halik, U. Zschieschang, G. n. Schmid, W. Radlik, and W. Weber, Journal of Applied Physics **92,** 5259 (2002).

[75] Y. Y. Lin, D. J. Gundlach, S. F. Nelson, and T. N. Jackson, Electron Device Letters, IEEE **18,** 606-608 (1997).

[76] M. X. Chen, E. Perzon, N. Robisson, S. K. M. Jonsson, M. R. Andersson, M. Fahlman, and M. Berggren, Synthetic Metals **146,** 233-236 (2004).

[77] A. Zen, J. Pflaum, S. Hirschmann, W. Zhuang, F. Jaiser, U. Asawapirom, J. P. Rabe, U. Scherf, and D. Neher, Advanced Functional Materials **14,** 757-764 (2004).

[78] M. Mottaghi and G. Horowitz, Organic Electronics: physics, materials, applications **7,** 528-536 (2006).

[79] M. J. Panzer and C. D. Frisbie, Advanced Functional Materials **16,** 1051-1056 (2006).

[80] G. Horowitz, R. Hajlaoui, D. Fichou, and A. E. Kassmi, Journal of Applied Physics **85,** 3202-3206 (1999).

[81] G. Horowitz, M. E. Hajlaoui, and R. Hajlaoui, Journal of Applied Physics **87,** 4456-4463 (2000).

[82] M. C. J. M. Vissenberg and M. Matters, Physical Review B - Condensed Matter and Materials Physics **57,** 12964-12967 (1998).

[83] L. Burgi, T. J. Richards, R. H. Friend, and H. Sirringhaus, Journal of Applied Physics **94,** 6129-6137 (2003).

[84] K. P. Puntambekar, P. V. Pesavento, and C. D. Frisbie, Applied Physics Letters **83,** 5539-5541 (2003).

[85] R. A. Street and A. Salleo, Applied Physics Letters **81,** 2887-2889 (2002).

[86] G. B. Blanchet, C. R. Fincher, M. Lefenfeld, and J. A. Rogers, Applied Physics Letters **84,** 296-298 (2004).

[87] A. Knobloch, A. Manuelli, A. Bernds, and W. Clemens, Journal of Applied Physics **96,** 2286-2291 (2004).

[88] G. H. Gelinck, T. C. T. Geuns, and D. M. d. Leeuw, Applied Physics Letters **77,** 1487-1489 (2000).

[89] A. Facchetti, M. H. Yoon, and T. J. Marks, Advanced Materials **17,** 1705-1725 (2005).

[90] M. Halik, H. Klauk, U. Zschieschang, G. Schmid, C. Dehm, M. Schutz, S. Maisch, F. Effenberger, M. Brunnbauer, and F. Stellacci, Nature **431,** 963-966 (2004).

[91] S. Chao and W. M. S., Journal of the American Chemical Society **109,** 6627-31 (1987).

[92] A. S. Dhoot, J. D. Yuen, M. Heeney, I. McCulloch, D. Moses, and A. J. Heeger, PNAS **103,** 11834-11837 (2006).

[93] I. N. Hulea, H. B. Brom, A. J. Houtepen, D. Vanmaekelbergh, J. J. Kelly, and E. A. Meulenkamp, Physical Review Letters **93,** 166601-4 (2004).

[94] D. Nilsson, M. Chen, T. Kugler, T. Remonen, M. Armgarth, and M. Berggren, Advanced Materials **14,** 51-54 (2002).

[95] M. J. Panzer and C. D. Frisbie, J. Am. Chem. Soc. **127,** 6960-6961 (2005).

[96] E. Said, X. Crispin, L. Herlogsson, S. Elhag, N. D. Robinson, and M. Berggren, Applied Physics Letters **89,** 143507 (2006).

[97] M. Taniguchi and T. Kawai, Applied Physics Letters **85,** 3298-3300 (2004).

[98] M. J. Panzer and C. D. Frisbie, J. Am. Chem. Soc. **129,** 6599-6607 (2007).

[99] A. Dodabalapur, Z. Bao, A. Makhija, J. G. Laquindanum, V. R. Raju, Y. Feng, H. E. Katz, and J. Rogers, Applied Physics Letters **73,** 142-144 (1998).

[100] K. L. Tzeng, H. F. Meng, M. F. Tzeng, Y. S. Chen, C. H. Liu, S. F. Horng, Y. Z. Yang, S. M. Chang, C. S. Hsu, and C. C. Chi, Applied Physics Letters **84,** 619-621 (2004).

[101] L. Zhou, A. Wanga, S. C. Wu, J. Sun, S. Park, and T. N. Jackson, Applied Physics Letters **88,** 083502 (2006).

[102] M. G. Kane, J. Campi, M. S. Hammond, F. P. Cuomo, B. Greening, C. D. Sheraw, J. A. Nichols, D. J. Gundlach, J. R. Huang, C. C. Kuo, L. Jia, H. Klauk, and T. N. Jackson, IEEE Electron Device Letters **21,** 534-536 (2000).

[103] Y. Watanabe, H. Iechi, and K. Kudo, Thin Solid Films **516,** 2731-2734 (2008).

[104] P. Andersson, R. Forchheimer, P. Tehrani, and M. Berggren, Advanced Functional Materials **17,** 3074-3082 (2007).

[105] Y. Chen, J. Au, P. Kazlas, A. Ritenour, H. Gates, and M. McCreary, Nature **423,** 136 (2003).

[106] B. Comiskey, J. D. Albert, H. Yoshizawa, and J. Jacobson, Nature **394,** 253-255 (1998).

[107] A. Kumar, A. Nathan, and G. E. Jabbour, IEEE Transactions on Electron Devices **52,** 2386-2394 (2005).